

Gold Nanostars Surface Enhanced Raman Spectroscopy (SERS) DNA Biosensor for TB Detection



Submitted by

Alavia Batool (323428)
Aleeza Shakeel (324393)
Ghazia Khalid (322764)
Syeda Aleena Abbas (324910)

Supervised By

Dr. Shah Rukh Abbas

Atta-Ur-Rahman School of Applied Biosciences (ASAB)

National University of Sciences & Technology (NUST)

(2023)

THESIS ACCEPTANCE CERTIFICATE

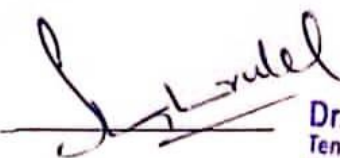
It is certified that the final copy of the BS FYP Thesis titled “Gold Nanostars Surface Enhanced Raman Spectroscopy (SERS) DNA Biosensor for TB Detection” submitted by Alavia Batool, Aleeza Shakeel, Ghazia Khalid, and Syeda Aleena Abbas of ASAB, NUST have been vetted by the undersigned, found complete in all respects as per NUST regulations and have been found satisfactory for the requirement of the degree.

Signature (Supervisor):

Dr. Shah Rukh Abbas

ASAB, NUST

Date:



Dr. Shah Rukh Abbas
Tenured Associate Professor
Dept of Industrial Biotechnology,
Atta-ur-Rahman School of Applied
Biosciences (ASAB), NUST Islamabad

Signature (HOD):

Dr. Amjad Ali

ASAB, NUST

Date:



Dr. Amjad Ali, PhD
Head of Department (HoD)
Industrial Biotechnology
Atta-ur-Rahman School of Applied
Biosciences (ASAB), NUST Islamabad

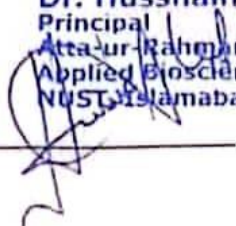
Signature (Dean/Principal)

Dr. Hussnain Ahmed Janjua

ASAB, NUST

Date:

Dr. Hussnain A. Janjua
Principal
Atta-ur-Rahman School of
Applied Biosciences (ASAB)
NUST Islamabad



AUTHOR'S DECLARATION

We, Alavia Batool, Aleeza Shakeel, Ghazia Khalid, and Syeda Aleena Abbas hereby state that our BS FYP thesis titled **"Gold Nanostars Surface Enhanced Raman Spectroscopy DNA Biosensor for TB Detection"** is our work and has not been submitted previously by us for taking any degree from the National University of Science and Technology (NUST) or anywhere else in the country/world.

At any time if our statement is found to be incorrect even after our graduation, the university has the right to withdraw our BS degree.


Name of student: Alavia Batool

Signature



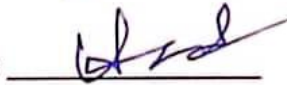
Name of student: Aleeza Shakeel

Signature



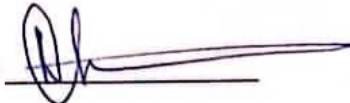
Name of student: Ghazia Khalid

Signature



Name of student: Syeda Aleena Abbas

Signature



CERTIFICATE FOR PLAGIARISM

It is to confirm that this BS thesis titled “Gold Nanostars Surface Enhanced Raman Spectroscopy (SERS) DNA Biosensor for TB Detection” by Alavia Batool (323428), Aleeza Shakeel (324393), Ghazia Khalid (322764) and Syeda Aleena Abbas (324910) has been examined by me. I undertake that,

1. The thesis has significant new work/knowledge as compared to already been published elsewhere. No sentence, table, equation, diagram, paragraph, or section has been copied verbatim from previous work except when placed under quotation marks and duly referenced.
2. The work presented is original and own work of authors i.e., there is no plagiarism. No idea, results, or works of others have been presented as the authors’ own work. There is no fabrication of data or results such that the research is not accurately represented in the records. The thesis has been checked using Turnitin, and a copy of the originality report is attached and focused within limits as per HEC plagiarism policy and instructions.



(Supervisor)

Dr. Shah Rukh Abbas

Tenured Associate Professor

ASAB, NUST

Dr. Shah Rukh Abbas
Tenured Associate Professor
Deptt of Industrial Biotechnology
Atta-ur-Rahman School of Applied
Biosciences (ASAB), NUST Islamabad

*Dedicated to our exceptional parents, teachers, and
adored siblings whose tremendous support and
cooperation led us to this wonderful accomplishment!*

ACKNOWLEDGEMENTS

In the name of Allah, the Most Gracious, the Most Merciful.

Alhamdulillah, all praise, and thanks to Allah Almighty, the Lord of the Worlds. It is with a profound sense of gratitude that we acknowledge His infinite blessings and guidance throughout our academic journey and the completion of this thesis.

We are deeply grateful to Allah for bestowing upon us the intellect, determination, and perseverance to undertake this research endeavor. His mercy and blessings have been a constant source of inspiration and strength, enabling us to navigate the challenges and complexities of the research process.

We would like to thank our principal **Dr. Hussnain Janjua** for providing us with this opportunity, and our supervisor **Dr. Shah Rukh Abbas** who continued to be a form of support, care, and backing to us in times of uncertainty throughout the various phases of our final year project. Her trust in our abilities made us work on this project confidently. Accept our heartfelt gratitude for your time, support, and patience.

We would like to take this opportunity to express our deepest gratitude and appreciation to our family and friends who have supported us throughout our academic journey and the completion of this thesis. Their unwavering encouragement, love, and understanding have been invaluable to us, and we are truly blessed to have such incredible individuals in our lives.

Most importantly, we would like to appreciate and acknowledge the countless hours our seniors **Mr. Muzammil Mujtaba Hashmi, Ms. Mushkbar Fatima, Mr. Nauman Javed and Miss Noor-ul- Ain**, have dedicated to proofreading our work, providing feedback, and offering valuable insights. Their attention to detail, constructive criticism, and suggestions have played a significant role in refining our thesis and enhancing its quality. Their input and perspectives have broadened our horizons and shaped our research in ways we could not have accomplished alone.

We would also like to acknowledge Scanning Electron Microscope Lab, Department of Materials Science and Engineering, Institute of Space Technology (IST), Islamabad; SNS instrumental lab, School of Natural Sciences (SNS), NUST; Advanced Energy Materials and Systems Lab,

USPCAS-E, National University of Sciences and Technology (**NUST**) for aiding in our research project.

We are grateful to Ms. Hina (**ASAB**) for her cooperation during the research project.

Finally, we would like to express our gratitude to all the individuals who have rendered valuable assistance to our final-year project.

As I conclude this acknowledgment, I am reminded of the verse from the Quran (Surah An-Nahl, 16:78), which states: "And Allah has extracted you from the wombs of your mothers not knowing a thing, and He made for you hearing and vision and intellect that perhaps you would be grateful." May Allah accept our humble efforts and make this thesis a means of benefit for others. All praise and thanks are due to Allah alone, the Lord of all creation.

Table of Contents

1. INTRODUCTION	14
1.1 Biosensor System	14
1.2 Biosensors and Nanotechnology in Diagnostics	15
1.2.1 SERS as Emerging Biosensing Technology	15
1.2.2 Advantages of SERS for Biomedical Analyses	15
1.3 Nanostructures.....	16
1.3.1 Nanoparticles in Biosensing	16
1.4 SERS based Biosensors for Infectious Disease Diagnosis.....	17
1.4.1 Tuberculosis	18
1.4.2 Conventional TB Detection Techniques	19
1.4.3 SERS-based Optical Biosensor for TB Diagnosis	19
1.5 Rationale.....	20
1.6 Aim of the project	20
1.7 Objectives.....	20
2. LITERATURE REVIEW	21
2.1 Surface Enhanced Raman Spectroscopy	21
2.2 Basic Principle of SERS.....	21
2.2.1 SERS Enhancement Mechanisms	22
2.3 SERS Substrates.....	23
2.3.1 SERS Substrates Based on Type of Nanoparticles	23
2.3.2 SERS Substrates Based on Shape of Nanoparticles	24
2.4 State of Art: SERS Sensors for Infectious Diseases	25
2.4.1 AuNSs as SERS Substrates.....	25
2.4.2 Conjugation Techniques for Substrate Attachment	25
2.4.3 DNA as a Receptor Molecule	27
3. METHODOLOGY	28
3.1 Chemicals	28
3.2 SERS Substrate Formation.....	28
3.2.1 Synthesis of Seed Solution.....	28
3.2.2 Synthesis of Gold Nanostars from the Pre-Formed Seed Solution.....	29
3.3 SERS Chip Preparation	30

3.3.1	Functionalization of Glass Slides with Thiol Groups	30
3.3.2	Attachment of Gold Nanostars on MPTMS Functionalized Glass Slides	30
3.3.3	Thiolated ss DNA Probe Attachment on Gold Nanostars Adsorbed Glass Slides ..	31
3.3.4	Analyte Attachment on the DNA Probe-Modified AuNSs Adsorbed Glass Slide ..	31
3.4	Overview of Methodology	33
3.5	Characterization Techniques	34
3.5.1	UV- Vis Spectrophotometry	34
3.5.2	Attenuated Total Reflectance - Fourier-transform Infrared Spectroscopy (ATR- FTIR)	34
3.5.3	Scanning Electron Microscopy (SEM)	34
3.5.4	Surfaced Enhanced Raman Spectroscopy (SERS)	34
4.	RESULTS	36
4.1	SERS Substrate Formation Conformation	36
4.1.1	UV-Vis Analysis	36
4.1.2	Scanning Electron Microscopy (SEM) Analysis.....	36
4.2	Confirmation of Glass Slide Functionalization with Thiol Groups.....	38
4.2.1	ATR-FTIR Analysis	38
4.3	Surface Enhanced Raman Spectroscopy (SERS) Analysis	38
4.3.1	SERS Spectra of Probe Modified Gold Nanostars Adsorbed Slide	38
4.3.2	Comparative SERS Analysis for Analyte Detection	39
4.3.3	Specificity of SERS DNA Biosensor	40
5.	DISCUSSION	42
6.	CONCLUSION.....	47
7.	FUTURE PROSPECTS	48
8.	REFERENCES	49

Table of Figures

Figure 1 Components of a typical biosensor. The bioreceptor recognizes the analyte while the transducer converts biological response into measurable signal. 14

Figure 2 Comparison of Raman Spectroscopy and SERS. (a) When incident laser light falls on analyte, a Raman scattering signal is produced. However, for SERS, the Raman scattering signal is enhanced due to adsorption of analyte on metallic nanostructures. 22

Figure 3 SEM images of three different types of gold nanoparticles based on their shapes. (a) Gold nanospheres (b) Gold nanotriangles (c) Gold nanostars. Image obtained from “Review of SERS substrate for chemical sensing” (Mosier-Boss P. A., 2017)..... 24

Figure 4 (a) Molecular Structure of MPTMS. (b) The terminal thiol group of MPTMS results in Au-S bond formation and three alkoxy groups contribute to Si-O bonding on glass substrate. Image obtained and modified from: MPTMS self-assembled monolayer deposition for ultra-thin gold films for plasmonics (Gothe et al., 2018)..... 26

Figure 5 a) Color change of the solution to violet – initial step b) Color change of the solution to red indicating seed formation c) Color change to deep blue showing gold nanostar presence d) Glass slide dipping in the gold nanostar colloidal solution. 29

Figure 6 SERS chips and controls. (a) Probe modified AuNSs adsorbed slide. (b) SERS chip with target analyte (TB DNA). (c) Control glass slide without SERS substrate. (d) SERS chip with non-target analyte (E. coli DNA) 32

Figure 7 Schematic diagram of methodology 33

Figure 8 UV-Vis absorption versus wavelength graph of gold nanostars with a broad absorbance peak at 664nm. 36

Figure 9 SEM images of gold nanostars where nanostars can be clearly seen in red circles having several branches and tips (a) Magnification 150 kx, scale 200nm. (b) Magnification 70.0 kx, scale 500 nm. (c) EDS analysis of powdered gold nanostars where Au confirms the presence of gold and Si and O correspond to the glass slide..... 37

Figure 10 FTIR analysis of MPTMS functionalized SiO₂ glass slides depicting different functional groups and bond stretching..... 38

Figure 11 SERS spectra of thiolated ss TB DNA probe modified gold nanostars in a wavelength range of 400-1600 cm^{-1} , indicating a sharp peak at 1083.89 cm^{-1} . The notation ν represents vibration stretching mode of C-S bond. 39

Figure 12 Raman spectra of analyte attached to ss thiolated probe acquired on (a) gold nanostars substrate (SERS Analysis) (b) simple glass slide without SERS substrate (Raman Analysis). The Raman intensity was effectively enhanced by using gold nanostars substrate ($6000-6500\ cm^{-1}$) which results in sensitive detection compared to that obtained without using gold nanostars as substrate ($4000-4500cm^{-1}$). 40

Figure 13 Specificity of thiolated ss DNA probe modified gold nanostars sensor towards TB DNA versus E. coli DNA. E. coli DNA showed no peaks whereas TB DNA provided enhanced Raman signal as evident by high Raman intensity..... 41

LIST OF ABBREVIATIONS

AuNSs	Gold Nanostars
CM	Chemical Enhancement
EM	Electromagnetic Enhancement
dd H ₂ O	Double distilled water
FTIR	Fourier Transform Infrared Spectroscopy
MPTMS	3-mercaptopropyl trimethoxysilane
PVP	Polyvinylpyrrolidone
SEM	Scanning Electron Microscope
SERS	Surface Enhanced Raman Spectroscopy
TB	Tuberculosis
UV-Vis	Ultraviolet-Visible Spectroscopy

ABSTRACT

Background: Surface Enhanced Raman Spectroscopy is a potent and unique spectroscopy technique for ultrasensitive sensing and trace detection of analyte adsorbed on the SERS substrate. Light driven technologies have contributed to improving the quality of life for centuries therefore an optical biosensor based on SERS technology using nanostructures as potential SERS substrate can be an effective, portable and sensitive analytical device for rapid diagnosis of infectious diseases. In current study, the potential of gold nanostars to exhibit high SERS spectra and ultra-sensitive detection against the target analyte (TB DNA) was evaluated.

Methodology: Gold nanostars were synthesized using seed mediated protocol and were characterized using UV-Vis spectroscopy and scanning electron microscope (SEM). MPTMS functionalized glass slides were coated with gold nanostars where thiol groups served as linkage moieties for immobilization process. Afterwards, single stranded thiolated DNA probes were drop casted onto the gold nanostars adsorbed glass slides. Eventually, SERS analysis was performed for the target (TB DNA) and non-target analyte (*E.coli DNA*) along with control group (without SERS substrate) to analyze the sensitivity of the sensor and for comparative analysis respectively.

Results: UV-Vis analysis revealed the distinct peak at 664nm attributed to gold nanostars whereas SEM analysis demonstrated the characteristic morphology of gold nanostars with sharp tips and branches. FTIR spectra of functionalized glass slides confirmed the glass coating via MPTMS through the presence of C-H bending, a characteristic of MPTMS. SERS spectra analysis against the target DNA resulted in high Raman intensity in comparison to non-target analyte (*E.coli DNA*) and control thereby successfully demonstrating the specificity and sensitivity of our SERS biosensor.

Conclusion: These findings suggest that gold nanostars serve as a potential substrate for the development of SERS based biosensors for more rapid, robust, specific and ultra-sensitive detection hallmark against and can be used for generating even more potent and versatile SERS sensors in the future.

Keywords: SERS, Raman intensity, Gold nanostars, Optical biosensor, Rapid disease diagnosis, TB DNA.

1. INTRODUCTION

1.1 Biosensor System

The term *biosensors* refer to an integrated analytical device that transduces the biochemical interactions between an analyte that needs to be detected with a biomolecule into optical, thermal, or electrical signal that is easily measured or quantified. In a biosensor, the bioreceptor (antibodies, enzymes, DNA, and even whole cells and microorganisms) is designed according to the specific analyte of interest to produce a response measured by a transducer. These analytical biosensors with biological sensing elements have acquired paramount importance in fields of diagnostics, biomedicines, drug discovery and delivery, environmental sustainability and food processing and safety (Srivastava et al., 2016). The working principle of a biosensor is illustrated in Fig. 1.

The first biosensor Clark electrode was invented in 1956 by Clark Jr. for the continuous detection of oxygen in blood during by-pass surgery. Glucometer, the first prototype of glucose sensor was also built by Clark in 1962. Biosensors as diagnostic tools need to fulfill certain requirements that are prerequisite to be as employed as efficient sensing devices like high sensitivity, selectivity, reproducibility, portability, chemical and mechanical stability. The objective of designing biosensors involves its advantages over conventional analytical methods such as miniaturization, portability, and minimal sample preparation (Filip et al., 2018).

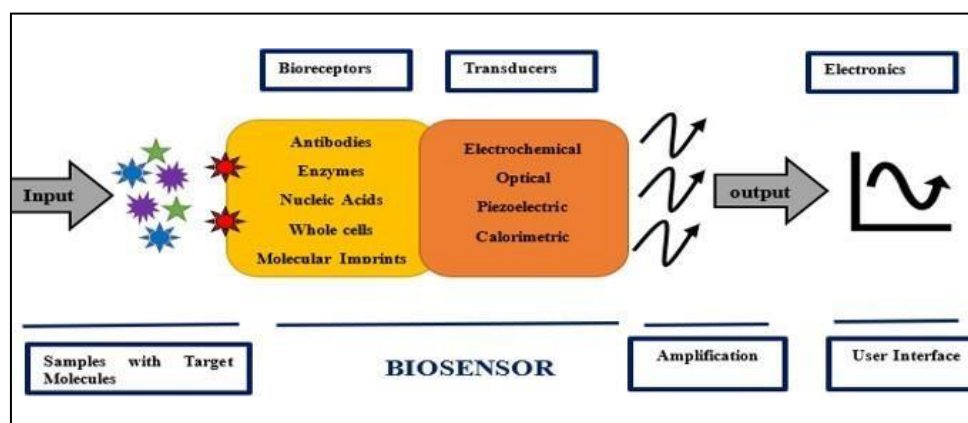


Figure 1 Components of a typical biosensor. The bioreceptor recognizes the analyte while the transducer converts biological response into measurable signal.

1.2 Biosensors and Nanotechnology in Diagnostics

Nanotechnology is well-known research filed presented by Nobel laureate Richard P. Feynman during his famous 1959 lecture, “*There’s a plenty of room at the bottom.*” (Feynman, 1992).

Since then, various revolutionary developments at the nanoscale have been made and thus played an increasingly important role in enhancing the sensitivity and specificity of biosensors at the nanoscale. Nanostructures have attracted the attention of researchers during the past few decades as excellent substrates for Surface Enhanced Raman Spectroscopy because of their characteristics and superior optical properties in comparison to bulk materials (Bellah et al., 2012; Botta et al., 2018). Biosensors using nanomaterials allow the use of new signal transduction technologies and rapid analysis of different molecules can be performed in-vivo, owing to their sub-micron size.

1.2.1 SERS as Emerging Biosensing Technology

The discovery of SERS 35 years ago became prominent when it was observed that the efficiency of Raman Scattering increases by 10^4 to 10^8 when it is aided by nanostructured metal surfaces. The Surface Enhanced Raman Scattering is a modification of Raman Scattering aided by metallic Nanoparticles. It is a powerful emerging biosensing technology that has shown great potential in the field of Diagnostics. This technology relies on the principle of utilizing the vibrational properties of metallic Nanoparticles to enhance the Raman Scattering of analytes. The prominent feature of SERS is that it can detect trace number of analytes with high specificity and selectivity. The ability of SERS to provide label-free and robust detection of analytes makes it an attractive technology for diagnostic purposes including drug delivery, early disease diagnosis and importantly, for monitoring therapeutic efficiencies. Moreover, the development of portable SERS devices to point-of-care diagnostics highlights the potential of this technology to revolutionize the field of diagnostics (Butler et al., 2016; Premasiri et al., 2005).

1.2.2 Advantages of SERS for Biomedical Analyses

SERS has been exploited in biomedical applications for the detection and identification of biomarkers. SERS offer several advantages for biomedical analyses as follows:

- Large increase in scattering cross-section permits the identification of diluted samples and analytes of low concentration in biological samples.
- SERS offers sensitivity to different molecular species in a complex mixture than Raman scattering.

- The competitive metal binding specificity of different molecular species selects for components over others and this selectivity attribute of SERS is highly applicable for biological mixture sample applications.
- Due to efficient energy transfer to the metal surface, fluorescence is effectively quenched in SERS than in Raman scattering.

Speed, enhanced sensitivity and specificity and fluorescence elimination provide the basis for SERS-based optical sensor solutions in clinical settings and biomedical applications (Butler et al., 2016).

1.3 Nanostructures

Nanostructures have gained prominence in the past few decades owing to high surface/volume ratio and ultra-small building units that impart nanostructures to exhibit characteristic specific properties including mechanical, optical, electronic, and magnetic properties. These plasmonic nanostructures are of great importance because their size can affect the physio-chemical properties of a substance. A wide range of diversity prevails in nanostructures ranging from nanoparticles to nanorods, nanoribbons, nanocages, and nanowires. Novel Nanomaterials in bioassay applications is a rapidly advancing field owing to their exceptional characteristics. These characteristics have made Nanostructures important in various application fields such as clinical diagnostics, biosensors, nanosensors, catalysis, solar cells, drug delivery, and forensic sciences (Jianrong et al., 2004).

1.3.1 Nanoparticles in Biosensing

Metallic noble nanoparticles have numerous applications in the development of biosensors. Functional Nanoparticles having optical and magnetic properties when bound to the biological molecules like enzymes, antibodies, DNA, proteins, and nucleic acids act as a biosensor that can be used to detect and amplify the signals generated by the transducer. Nanoparticle based biosensors include optical biosensors, piezoelectric biosensors, magnetic biosensors, and electrochemical biosensors.

Plasmonic Nanoparticles particularly Gold and Silver are most important during the development of optical biosensors as these are known to generate localized surface plasmon resonance (LSPR) which is exploited in SERS to amplify the intrinsically weak Raman Signal for analyte detection.

The LSPR and SERS enhancement can be modulated by changing the size, shape, and composition of the nanoparticles. In SERS based sensing applications these plasmonic nanoparticles act as efficient SERS substrates to produce high SERS enhancement factor, thereby contributing to analytical sensitivities (De Silva Indrasekara et al., 2018; Indrasekara et al., 2014).

1.4 SERS based Biosensors for Infectious Disease Diagnosis

Diagnosis is the key component for the eradication of infectious disease to improve global health. Accurate and early diagnosis of infectious diseases, particularly vector-borne and bacterial infections is crucial for effective disease management and to prevent deadly epidemics. Infectious diseases caused by parasites, bacteria, mosquito-borne and viruses and fungi are responsible for 15 million deaths each year accounting for 95% deaths in under-developing countries. Early diagnosis is critical and challenging because of low concentration of biomarkers and demanding bioanalytical techniques that can provide high sensitivity and ensured specificity. This emphasizes the urge to develop robust diagnostic techniques with highly sensitive detection capabilities that can revolutionize the diagnostics field and thereby, providing analytical tools for early biomolecules detection.

Current diagnostic techniques include highly sensitive Polymerase Chain Reaction (PCR) which has quite technical challenges and is expensive for implementation in resource-limited settings. Light microscopy based cytological examination is another diagnostic modality with high specificity but has one drawback of having poor sensitivity (Caliendo et al., 2013).

The gold standard method for diagnosing bacterial infections is cell-culture method which is time-consuming and slow. It may take 24 hours or more for fastidious organisms to culture a bacterial pathogen and sometimes 24-48 hr. (or longer) for antimicrobial susceptibility to be determined. This results in the physicians prescribing broad-spectrum antibiotics that kill large range of different micro-organisms until the culture results arrives and this practice is undoubtedly one of the major reasons of increasing prevalence of drug-resistant bacteria (Caliendo et al., 2013).

Due to prolonged diagnostic period of bacterial detection, antibiotics are prescribed based on the presentation symptoms contributing to ineffective treatment, chronic infections, and proliferation of multi-drug resistant bacteria. In light of this, there is a need to develop robust, cost-effective, and highly sensitive and specific and portable diagnostic tools that can extend to point-of-care applications (Hamm et al., 2019).

Owing to the inherent optical and chemical properties of noble plasmonic nanoparticles, when combined with Raman Spectroscopy resulted in a powerful analytical tool *SERS* which is Surface Enhanced Raman Scattering; particularly advantageous for diagnostic purposes and has emerged as new detection modality because SERS has the potential to meet the unmet biomedical need for the rapid and specific detection of bacterial cells present in the complex human body fluids (Caliendo et al., 2013).

1.4.1 Tuberculosis

Tuberculosis (TB) is among the oldest human diseases with a high mortality rate in Third World developing countries, owing to poverty, poorly ventilated and over-crowded conditions. TB is a contagious bacterial airborne disease that causes people in severe poverty to get infected by this deadly bacterium due to working in crowded places with poor ventilation, resulting in the progression of the disease. The causative agent of TB is *Mycobacterium Tuberculosis* primarily affects the lungs, but it can also affect other organs such as the brain, spine, and kidneys. The global incidence of TB is 10.6 million people each year as reported by the World Health Organization (WHO) (Chakaya et al., 2021).

TB is endemic in many low- and middle-income countries, with the highest burden of disease in Africa and Southeast Asia. According to the WHO, there were an estimated 10 million cases of TB worldwide in 2019, with 1.4 million deaths (Chakaya et al., 2021). In terms of risk factors, TB primarily affects people with weakened immune systems, such as those living with HIV/AIDS, people who smoke tobacco, people with malnutrition, and people living in crowded or poorly ventilated conditions. TB is also more common in certain age groups, with the highest incidence among adults aged 25-44 years. Detection of TB is a major problem as the majority of people being co-infected with another deadly virus HIV which is 60% of the cases. Currently, TB diagnosis is a major concern; with the majority of TB patients being sputum scarce (including HIV coinfecting patients), others being smear-negative (low concentration of TB bacteria in the sputum). However, early diagnosis of TB can help prevent the propagation of the bacteria (Chakaya et al., 2021).

1.4.2 Conventional TB Detection Techniques

There exists a variety of conventional diagnostic procedures for the diagnosis of TB bacteria with varied limitations in test duration, sensitivity, accuracy, and diagnostic expenses. The standard diagnostic test for Tuberculosis includes fluorescent staining and Ziel-Neelsen Staining. Simple Microscopy is generally simple but lacks sensitivity. Similarly, the Sputum Culture Test accurately identifies *Mycobacterium tuberculosis* through the sputum sample of infected patients. Despite high- specificity, it takes almost 1 to 8 weeks for the sputum culture to grow and requires specialized workers and a BSL-2 facility. The Nucleic Acid Amplification NAA test due to its high specificity to confirm positive sputum smear makes it a more accurate diagnostic test but it shows limitations toward extra-pulmonary TB. Recent advancements in molecular diagnostics have made it possible to develop a DNA or peptide-based biosensor to detect TB directly from the specimens. Therefore, rapid, and accurate diagnosis of TB is crucial to accelerate treatment efficacy and mitigate disease progression (Wolinsky, 1994).

1.4.3 SERS-based Optical Biosensor for TB Diagnosis

Light-driven technologies have contributed to improving the quality of life for centuries. In the past few decades, light-based technologies over-employed materials have been used for advancement in the fields of medicine and energy. In light of this, a new research field “*Plasmonics*” has emerged. For TB diagnosis, an optical biosensor based on SERS technology and gold nanoparticles as a SERS substrate can be an effective and highly sensitive analytical tool for diagnosis. An optical biosensor consists of a gold-coated glass slide onto which the insertion sequence is adsorbed. It works on the principle of LSPR which is Localized Surface Plasmon Resonance. For LSPR, gold nanoparticles have received special attention due to their chemical inertness and synthetic accessibility. Anisotropic AuNPs (stars, cubes, cages) are superior to spherical AuNPs due to high electric field enhancements at sharp edges and tips rendering them as efficient plasmonic substrates for Surface Enhanced Raman Spectroscopy. When an incoming light falls onto the metal surface, the free electrons undergo coherent oscillations. When such oscillations are restricted to a metal-dielectric interface and light interacts with the particles much smaller than its wavelength, it results in the generation of LSPR, and the resulting optical signal is converted by the transducer for analytical purposes. Therefore, the development of such biosensors will result in more robust, rapid, highly specific, and sensitive detection for TB diagnosis.

1.5 Rationale

Since the conventional diagnostic biosensors have limitations including long durations to detect tuberculosis, need infrastructure, requiring a technician to operate, etc., thus we propose a robust and sensitive optical SERS DNA biosensor solution to serve humanity.

1.6 Aim of the project

This project aims to synthesize gold nanostars and determine if they have the potential to be used as SERS substrates to detect tuberculosis disease.

1.7 Objectives

The main objectives are:

1. Selection of nanoparticles that show the best SERS response through literature review.
2. Synthesis of SERS substrate (gold nanostars) & attachment of these gold nanostars to functionalized glass slides.
3. Functionalization of gold nanostars modified glass slides with thiolated DNA Probes.
4. Morphological Characterization of substrate & SERS Analysis of analyte (TB DNA).

2. LITERATURE REVIEW

2.1 Surface Enhanced Raman Spectroscopy

Surface Enhanced Raman Spectroscopy is a powerful and unique spectroscopy technique for ultrasensitive sensing and trace detection of analyte adsorbed on the SERS substrate i.e. on the surface of metallic nanoparticles or roughened metallic surfaces (Betz et al., 2014; Deng et al., 2018; Liu et al., 2021; Pérez-Jiménez et al., 2020). The use of noble metallic nanomaterials as substrates amplify the Raman scattering intensity of the analyte by 6-8 times, thereby enabling SERS to detect the concentration of an analyte as low as that of a single molecule and thus overcoming the disadvantage of low sensitivity as seen with conventional vibrational Raman Spectroscopy (Liu et al., 2021).

Owing to its intrinsic specificity for molecular fingerprinting and the characteristic ability for single-molecule detection, SERS has become a hot research field in various areas of science including physics, chemistry, life sciences, biomedicine, and nanotechnology. Particularly in the field of biology, SERS has emerged as one of the most promising techniques that not only detect trace amounts of biological molecules such as DNA, proteins, or micro RNAs but also provides valuable structural insight of biological analytes along with bioimaging and diagnosis of infectious diseases (Liang et al., 2021).

2.2 Basic Principle of SERS

Like Raman Spectroscopy, the phenomenon of Surface Enhanced Raman Spectroscopy is based on inelastic collision and scattering of incident laser light, whereupon interaction of light photons with the vibrational state of molecules, the frequency of incident light changes, and spectral peaks are obtained. However, the characteristic distinguishing feature of SERS is that it is aided with metallic nanostructures, and upon adsorption of targeted molecules on these metallic nanoparticles, the Raman scattered signals from target molecules are enhanced by several orders of magnitude as shown in Fig. 2 (a, b) that allow for detection of the ultra-low concentration of analyte and sometimes even a single molecule- limitation of Raman Spectroscopy (Petersen et al., 2021).

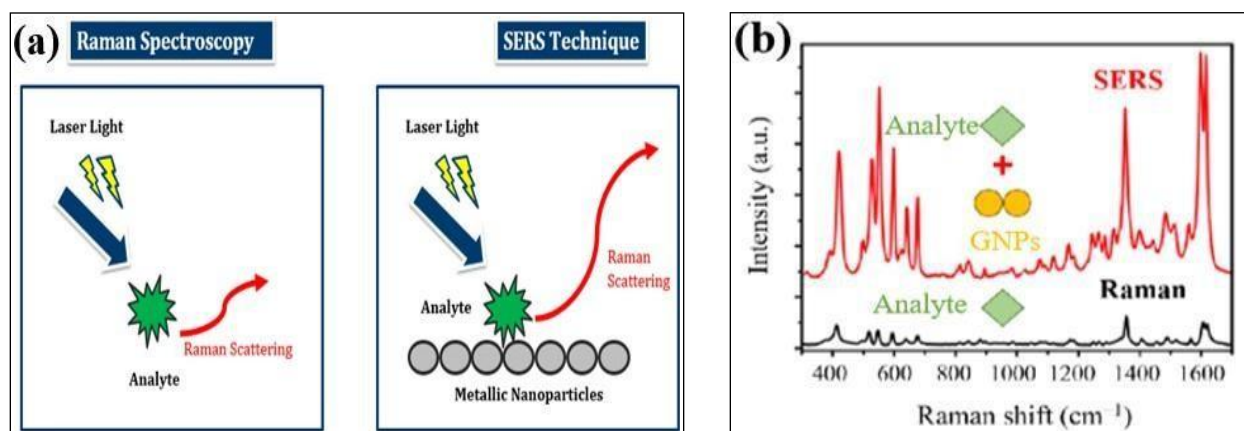


Figure 2 Comparison of Raman Spectroscopy and SERS. (a) When incident laser light falls on analyte, a Raman scattering signal is produced. However, for SERS, the Raman scattering signal is enhanced due to adsorption of analyte on metallic nanostructures.

2.2.1 SERS Enhancement Mechanisms

The enhancement of Raman Signal is largely based on two main mechanisms: Electromagnetic (EM) and Chemical enhancement (CE).

Electromagnetic enhancement is the predominant contributor to enhanced SERS response that is due to a substrate (metallic nanoparticles) and occurs when the frequency of the incident light resonates with the frequency of the collectively oscillating metallic nanoparticles' conduction band electrons i.e., localized surface plasmon resonance (LSPR). Furthermore, hotspots (the regions or the gaps when two nanostructures are near each other) contribute a strong field enhancement that is localized around metallic nanoparticles interface and causes the adsorbed molecule to act as a point dipole and further enhance the efficiency of the scattered light. As a result, the SERS enhancement contribution by EM is up to 10^{10} times and this EM depends largely on substrate morphology and roughness thus making it independent of the nature and type of molecule (Saviñon-Flores et al., 2021; Edinburgh Instruments Ltd., 2023).

Chemical Enhancement occurs due to the charge transfer between metallic substrate conduction band electrons and the lowest unoccupied orbital of the adsorbed molecule. CE has a much smaller effect compared to EM, typically around 10^2 to 10^4 . It requires metal nanoparticles and molecules to be nearby so that electrons can be transferred to and from metallic nanostructures thus changing the polarizability of adsorbed molecules. During this electron transfer, a negative ion is formed, and Raman signal enhancement is maximum when it resonates with the same energy as that of the

incident photon. Unlike EM, CE mainly depends on the bonding and geometry of the adsorbed molecule. (Kumar et al., 2020; Saviñon-Flores et al., 2021; Edinburgh Instruments Ltd., 2023).

2.3 SERS Substrates

SERS substrates are any of the metallic nanoparticles or nanostructures that can enhance the Raman signal and ultimately SERS response by supporting the LSPR phenomenon. SERS active substrates are mainly classified into three categories as mentioned by (Mosier-Boss P. A., 2017):

- a. Metallic nanoparticles in colloidal solution/suspension
- b. Metallic nanoparticles deposited on solid surfaces e.g. glass, paper, alumina, quartz, etc.
- c. Metallic nanostructures that are fabricated on solid surfaces using nanofabrication techniques such as nanolithography or electron beam lithography

The characteristics of an ideal SERS substrate are that it should not only enhance SERS response by amplifying the Raman signal but also provide uniform enhancement throughout the surface in addition to being stable, reproducible, and cost effective (Edinburgh Instruments Ltd., 2023). Although colloids, one of the most widely used SERS substrates, are easily prepared in laboratories and can enhance the Raman signal manifold, their instability along with their inhomogeneous nature and poor reproducibility, a consequence of Brownian motion of particles in colloidal solution limit their application (Saviñon-Flores et al., 2021). Similarly, nanofabrication techniques such as nanolithography for obtaining organized arrays of metallic nanoparticles on solid surfaces are one of the most powerful used techniques for making the best SERS substrates. But the overall process is slow and time-consuming and the high cost associated with expensive equipment further hampers the use of such techniques for making SERS substrates (Kumar et al., 2020). In comparison, metallic nanoparticles deposited on solid substrates are stable, provide significant enhancement of the Raman signal, and cost efficient compared to nanolithography procedures.

2.3.1 SERS Substrates Based on Type of Nanoparticles

The magnitude of SERS enhancement depends on metallic nanoparticles type, size, shape and the number of hotspots (Mosier-Boss P. A., 2017). When it comes to the type of nanoparticles, coinage metals including gold, silver and copper have shown promising SERS effect and enhancement of Raman signal compared to some other transition metals such as iron and platinum, thus limiting the use of later ones as SERS active substrates (Kumar et al., 2020). Among these coinage metals, gold and silver are mostly preferred on copper because of their ability to create a strong plasmonic

effect, inert nature and most importantly potential to form well composed nanostructures (Cong et al., 2020). Furthermore, the plasmon resonance frequencies of both these nanoparticles lie within visible and near infrared regions which are well suited because the wavelength in Raman spectroscopy lie in a similar range. However, silver too, has a major drawback that it is easily oxidized and has a potential to react with atmospheric sulfur compounds. Therefore, among the coinage metals, gold is highly preferred for use as SERS active substrate because of its inert nature, low toxicity and ability to create a strong plasmonic effect (Kumar et al., 2020).

2.3.2 SERS Substrates Based on Shape of Nanoparticles

SERS is not only influenced by the type and composition of nanoparticles (i.e., gold, silver, copper) but also by the size and shape of these nanostructures. Nanoparticles shape is controlled by surfactants that permit defined growth by stabilizing certain crystal planes. Thus, nanoparticles can acquire particular shapes i.e., rod shape (nanorods), triangular shape (nanotriangles), cage shape (nanocages), star shaped (nanostars) etc. as shown in Fig. 3 depending on the type of surfactant used (Mosier-Boss P. A., 2017).

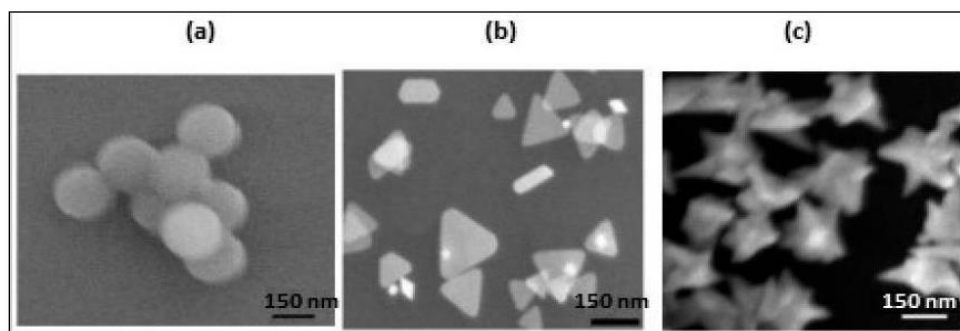


Figure 3 SEM images of three different types of gold nanoparticles based on their shapes. (a) Gold nanospheres (b) Gold nanotriangles (c) Gold nanostars. Image obtained from “Review of SERS substrate for chemical sensing” (Mosier-Boss P. A., 2017).

When it comes to shape of nanostructures, SERS response generally follows the following trend nanospheres < nanotriangles << nanostars. This is due to many branches and sharp tips or spikes (also known as nanoantennas) of nanostars that hotspots are increased and such nanostructures exhibit large local electromagnetic fields or LSPR and thus act as an interesting platform for biosensing and diagnostic purposes (Mosier-Boss P. A., 2017).

Since theoretical data established that nanostars are ideal candidates for carrying out SERS related studies therefore, gold nanostars (AuNS) serve as one of the best candidates owing to their great potential for plasmonic biosensing compared to nanorods, nanotriangles, nanoshells and hollow nanospheres.

2.4 State of Art: SERS Sensors for Infectious Diseases

2.4.1 AuNSs as SERS Substrates

Nanoparticles can be synthesized by both physical and chemical methods. SERS active substrates can be synthesized by wet chemical synthesis where gold ions in aqueous solution are reduced by reducing agents such as sodium citrate whose concentration and strength directly influence size of nanoparticles (Mosier-Boss P. A., 2017).

When it comes to defining shapes of nanoparticles i.e., nanospheres, nanorods, nanostars, nanocages etc., generally three methods are followed. One is a single step method also known as one pot synthesis in which metallic precursor and reducing agent both are added in a single step so that nucleation and growth takes place in a single reaction. However, this method has a major disadvantage that polydisperse nanoparticles are formed. The other one is the 2-[4-(2-hydroxyethyl) piperazin-1-yl] ethane sulfonic acid (HEPES) mediated AuNSs protocol. Compared to it, the other method i.e., seed-mediated growth of nanoparticles results in more stable nanoparticles that are monodispersed as well. Basically, in this method, pre-formed seeds act as nucleation points and growth occurs along them in the second step where certain chemicals (surfactants and capping agents) are added to direct and control the synthesis of desired shape. In case of AuNSs, silver nitrate (AgNO_3) is the chemical that comes into play to direct the formation of star shaped by forming branches around the central core (Phiri et al., 2019).

2.4.2 Conjugation Techniques for Substrate Attachment

Immobilization of gold nanoparticles on solid surfaces, for example glass can be achieved by both physical and chemical methods. Chemical methods usually involve the use of certain organic groups, such as amine and thiols which serve as linker molecules to form highly organized self-assembled monolayers (SAM) of nanoparticles onto the solid surfaces (Weinrib, H. et al., 2012). These linkage reagents not only ensure that gold nanoparticles are anchored on solid surfaces but also provide stability for longer durations.

APTES (3-aminopropyl triethoxysilane) is one of the frequently used linkage reagents that ensures the immobilization of gold nanoparticles on solid surfaces via electrostatic interaction between negatively charged gold nanoparticles and its amine groups whereas its ethoxy groups contribute silane anchorage to solid surfaces. However, it has been reported in several studies that these electrostatic interactions result in weak interactions and therefore, a more effective approach to adsorb gold nanoparticles on a solid surface is using thiol-based reagents that form strong covalent bond thereby resulting in much stronger interactions (Rao et al., 2019).

Organosilanes such as MPTMS (3-mercaptopropyl trimethoxysilane) are best known for forming strong covalent bonds between Au-S (bond strength of approximately 45 kcal/mol) thereby immobilizing gold nanoparticles on solid surfaces such as glass. Basically, the alkoxy groups of MPTMS contribute the formation of Si-O bonds by reacting with hydroxyl groups on glass slides (thereby adhering MPTMS on glass), and thus provide the functional thiol groups for reacting with AuNPs to form stable Au-S bond as shown in Fig. 4 (b) which on the other hand is also favored by the strong affinity of gold for thiol groups (Rao et al., 2019). Furthermore, in addition to the unique physical and chemical properties of these thiol linkage reagents, it is due to their excellent performance, long term stability, easy preparation that they serve as attractive candidates for gold-based SERS substrates adsorption on solid surfaces (Weinrib, H. et al., 2012).

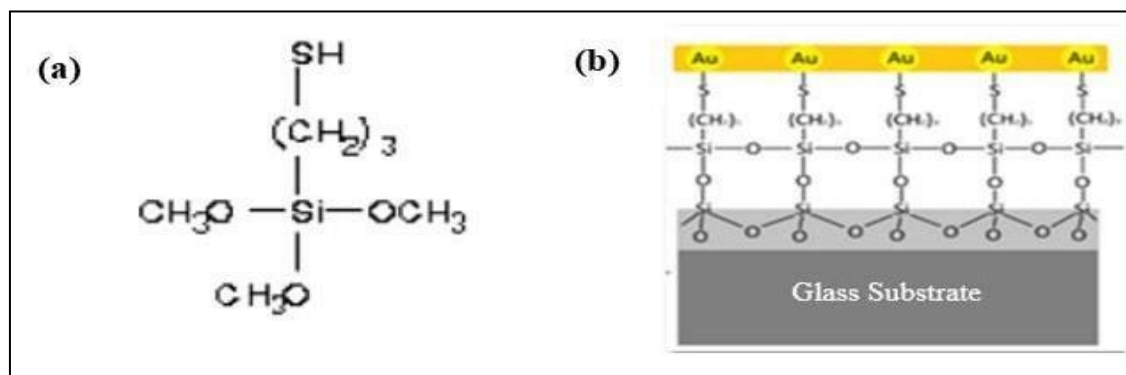


Figure 4 (a) Molecular Structure of MPTMS. (b) The terminal thiol group of MPTMS results in Au-S bond formation and three alkoxy groups contribute to Si-O bonding on glass substrate. Image obtained and modified from: MPTMS self-assembled monolayer deposition for ultra-thin gold films for plasmonics (Gothe et al., 2018).

2.4.3 DNA as a Receptor Molecule

Single stranded DNA probe immobilization on the surface of gold nanoparticles is an integral part in the construction of SERS chip. Different immobilization strategies have been used by researchers to achieve a highly organized probe layer on SERS substrates. One such approach is to modify one end of probe by adding functional groups such as thiol (SH). The probe can be labelled either directly with thiol groups or adding alkyl chains with sulfhydryl groups. This thiol modified ss DNA probe has a high affinity for binding with gold nanostructures through a strong covalent bond. The sulfur groups adsorb onto metallic nanostructures from solution thus resulting in immobilization of DNA probe on SERS substrates (Pyrak et al., 2019).

For SERS analysis on solid substrates, analyte is usually drop-casted on the surface of SERS chip and SERS measurement is carried out after providing adequate time for sample to dry on solid substrate (Saviñon-Flores et al., 2021). This addition of analyte to its complimentary ss DNA probe results in hybridization which is followed by changes in intensity of characteristic Raman bands and hence provides a characteristic SERS spectrum (Pyrak et al., 2019).

3. METHODOLOGY

3.1 Chemicals

Materials that were crucial to answer our research question and were used after doing a thorough literature search are 1g gold salt (Merck, Germany), hydrochloric acid (HCl) (31.5-32.5%) stock solution (BDH Laboratory Supplies, England), polyvinylpyrrolidone (PVP) (M.W. 40,000 \geq 99%) (VWR Chemicals, U.S.A), L-ascorbic acid (C₆H₈O₆) (PhytoTechnology Laboratories, U.S.A), silver nitrate (AgNO₃) (Sigma-Aldrich, U.S.A), trisodium citrate (Na₃C₆H₅O₇) (Sigma-Aldrich, Co., U.S.A), 3-mercaptopropyl trimethoxysilane (MPTMS) (Shanghai Macklin Biochemical Co., Ltd., China), ethanol (C₂H₅OH) (Sigma-Aldrich, Co., USA) & deionized water (Vitro Diagnostic Laboratories, Pakistan). All the glassware was washed with aqua regia to reduce the maximum level of contamination.

3.2 SERS Substrate Formation

3.2.1 Synthesis of Seed Solution

The gold nanostars were synthesized using the seeded AuNSs technique in which Turkevich-citrate reduction method was first used to prepare gold nanoparticles seeds and these pre-formed seeds were further used for nanostars synthesis. This protocol was modified further and optimized to get accurate results. Firstly, 0.25 mM HAuCl₄ solution was made and added to a beaker with 50 ml ddH₂O. This solution was heated up to 80°C on a hot plate (Velp Scientifica, F20500162). Side by side, 1% (w/v) trisodium citrate solution was prepared from which 1300 μ l was pipetted out and added to the heating solution (Phiri et al., 2019).

On increasing the temperature, the solution changed its color various times starting from violet as shown in the Fig. 5 (a) and turning the solution red in the end as shown in Fig. 5 (b). Trisodium

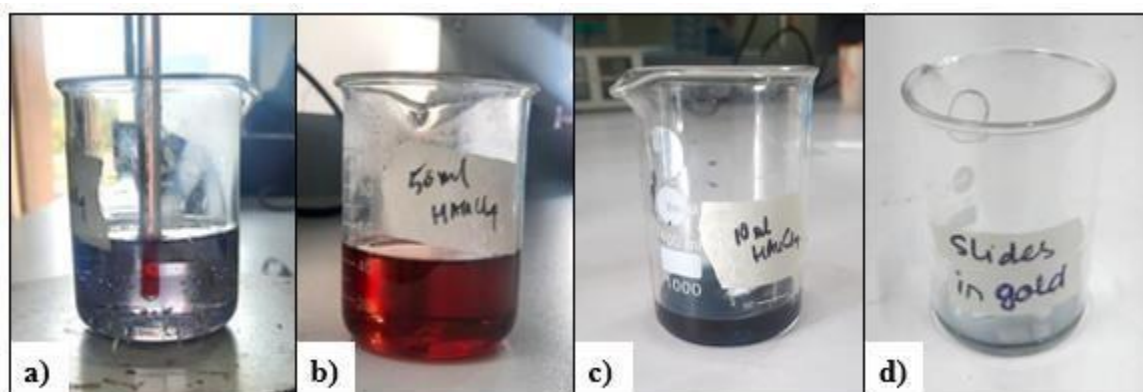


Figure 5 a) Color change of the solution to violet – initial step b) Color change of the solution to red indicating seed formation c) Color change to deep blue showing gold nanostar presence d) Glass slide dipping in the gold nanostar colloidal solution.

citrate addition was the marker step as it aids in seed formation. This seed solution was stored in the refrigerator at 4°C for further usage and to create batches of AuNSs.

3.2.2 Synthesis of Gold Nanostars from the Pre-Formed Seed Solution

For gold nanostars synthesis, 10 ml of 0.25 mM HAuCl₄ was added in a beaker and acidified by adding 10 µl 1 M HCl. Afterwards, 5 µl seed solution was pipetted out and added to the aforementioned beaker immediately. This beaker was then placed on a magnetic stirrer (Velp Scientifica, F20500162) followed by the simultaneous addition of 50 µl of 10 mM AgNO₃ and 50 µl of 100 mM ascorbic acid under mild stirring. The addition of these chemicals instantaneously resulted in a deep blue color change as shown in Fig. 5 (c). For the final step, 350 µl of 2.5 mM PVP was added to the solution to restrict the AuNSs' shape (Phiri et al., 2019).

The solution was then distributed equally in the 10 eppendorfs (each with 1 ml solution) which were then placed in a centrifuge (Eppendorf, 5415 R) for two hours at 3000g. After centrifugation, the supernatant was discarded and the pellets obtained were resuspended in 1ml double distilled water (Phiri et al., 2019).

Half of these pellets were used for ultraviolet (UV) and scanning electron microscope (SEM). The other half was used to dip the glass slides in their colloidal solution for substrate formation.

3.3 SERS Chip Preparation

3.3.1 Functionalization of Glass Slides with Thiol Groups

For functionalization of glass slides with thiol groups, the protocol to obtain self-assembled monolayers of MPTMS was followed with minor modifications. First of all, glass slides were cut equally by a glass cutter and then placed in an ethanol solution for 30 minutes. For the washing step, slides were removed from ethanol solution and added to a beaker with deionized water which was then sonicated in an ultrasonic cleaner (Huanghua Faithful Instrument Co., Ltd., FSF-010S) three times for five minutes. The deionized water was discarded after every five-minute wash and new deionized water was added. Side by side, to prepare a silane solution containing 3-mercaptopropyl trimethoxysilane, 1 ml MPTMS was added in 95% ethanol-water solution (v/v) (solution with 8.5 ml ethanol and 0.45 ml water respectively) so that the final concentration was 10% (Huang et al., 2009). In this freshly prepared silane solution, glass slides were submerged for 3 hours at room temperature.

After 3 hours, the slides were washed six times with ethanol from both sides. Later on, the slides were placed in the drying oven (Huanghua Faithful Instrument Co., Ltd, 101-1AB) at 110°C for 10 minutes to initiate the crosslinking step. Finally, the slides were saved in the desiccator with vacuum, to save the thiol bonds attached (Huang et al., 2009).

To check the functionalization of slides with thiol groups (MPTMS), the samples were sent to the Advanced Energy Materials & Systems Lab (USPCASE, NUST) for Attenuated Total Reflectance - Fourier Transform Infrared Spectroscopy (ATR-FTIR) analysis.

3.3.2 Attachment of Gold Nanostars on MPTMS Functionalized Glass Slides

The stored gold nanostar pellets were sonicated in an ultrasonic cleaner (Huanghua Faithful Instrument Co., Ltd., FSF-010S) for 10 minutes prior to the attachment step to bring the AuNSs into their colloidal state. Colloidal AuNS solution from eppendorfs was transferred to a small beaker and functionalized slides from the previous step were subjected to this solution overnight as shown in Fig. 5 (d). Later on these slides were washed with deionized water and air-dried. (Parmigiani et al., 2022).

3.3.3 Thiolated ss DNA Probe Attachment on Gold Nanostars Adsorbed Glass Slides

In order to attach the *Mycobacterium tuberculosis* analyte on the glass slides, the (IS)6110 insertion sequence probe which is exclusive for the *Mycobacterium tuberculosis* complex, was prepared by using TE buffer (pH 7) and stored at -20°C. From the prepared probe solution, 4 µl was pipetted out and drop-casted on the gold nanostars adsorbed thiol functionalized glass slides as shown in Fig. 6 (a). The slides were left for 1 hour and allowed to air dry. This step created the complete SERS chip. The DNA probe will act as a receptor to the analyte attached to it in the next step.

From SERS analysis, one of these slides was sent to the Raman Spectroscopy Lab at the School of Natural Sciences, NUST to confirm whether the DNA probe was successfully attached to gold nanostars modified glass slide or not. Furthermore, the remaining probe modified slides were used for target-analyte detection (TB DNA); and comparison studies by adding non-target analyte (*E. coli* DNA).

3.3.4 Analyte Attachment on the DNA Probe-Modified AuNSs Adsorbed Glass Slide

A dilution of 98µl TE buffer and 2 µl inactive tuberculosis DNA (obtained from Nanobiotechnology Lab, ASAB) was made. 4 µl of the solution was pipetted out from the freshly prepared buffer DNA dilution and drop-casted on the slide (from the previous step) with the DNA probe attached. This slide (analyte added to thiolated ss DNA probe modified gold nanostars adsorbed glass slide) as shown in Fig. 6 (b) was allowed to rest for 45 minutes at room temperature and sent to the Raman Spectroscopy Lab at the School of Natural Sciences, NUST for SERS analysis.

For control, a bare glass slide without any modification with SERS substrate (gold nanostars) was used as shown in Fig. 6 (c). The thiolated single-stranded DNA probe was attached to it directly and afterwards analyte (TB DNA) was added to it and air dried following the sample procedure as that of analyte attachment to complete SERS chip (the one modified with gold nanostars). This was done to compare the results and check the potential of AuNSs as a SERS substrate.

Moreover, to check the specificity of our SERS sensor, one of the probes modified gold nanostars adsorbed glass slide was taken, and on this slide, non-target analyte (*E. coli* DNA) was added

(following the same procedure for analyte attachment) instead of the target analyte (TB DNA) as shown in Fig. 6 (d). Both these slides were also sent to the Raman Spectroscopy Lab at the School of Natural Sciences, NUST, for SERS analysis.

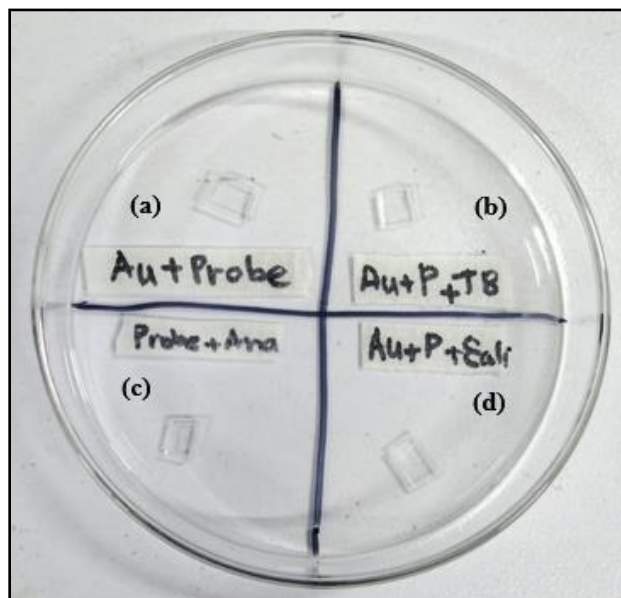


*Figure 6 SERS chips and controls. (a) Probe modified AuNSs adsorbed slide. (b) SERS chip with target analyte (TB DNA). (c) Control glass slide without SERS substrate. (d) SERS chip with non-target analyte (*E. coli* DNA).*

3.4 Overview of Methodology

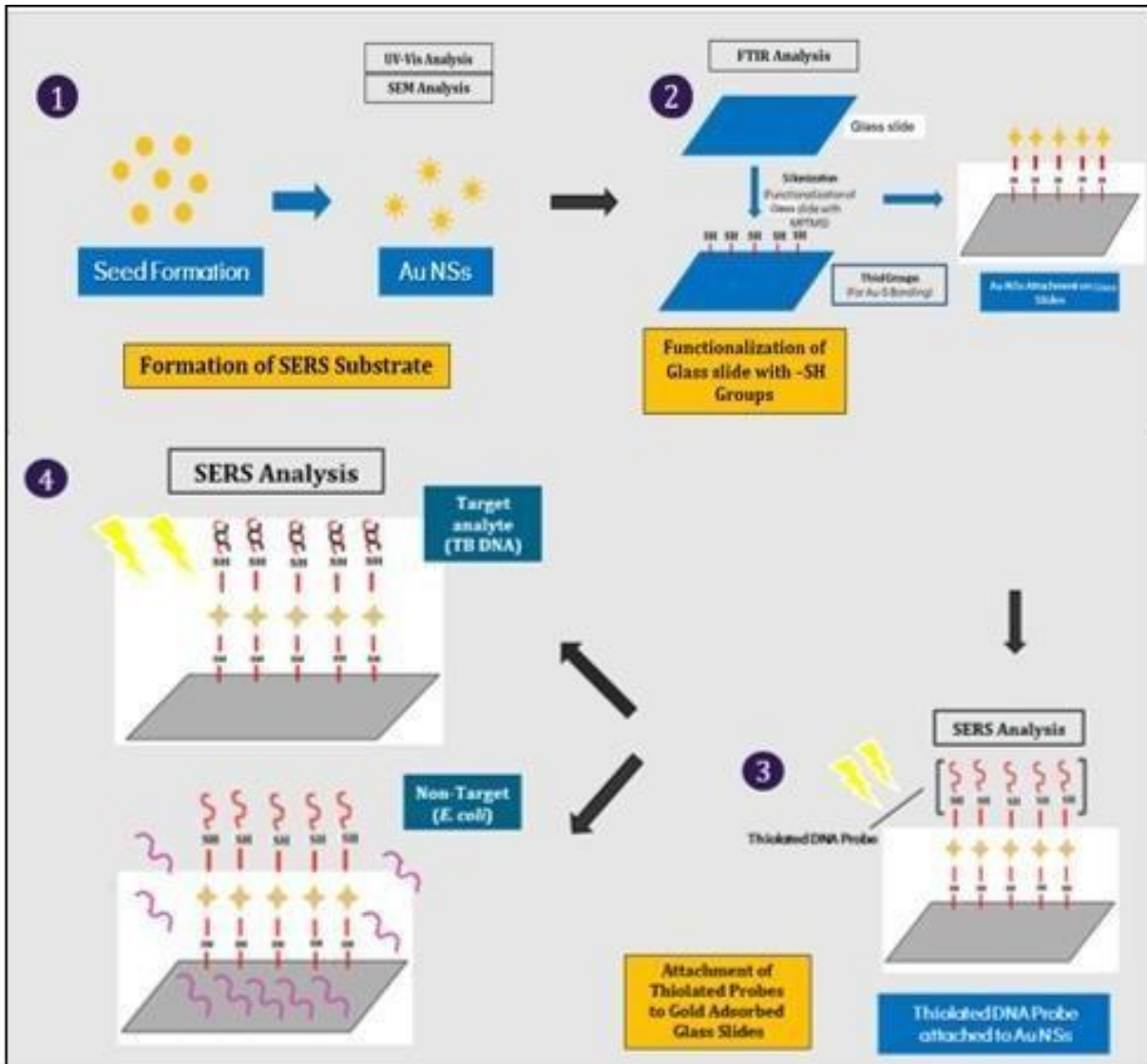


Figure 7 Schematic diagram of methodology

3.5 Characterization Techniques

3.5.1 UV- Vis Spectrophotometry

UV-Vis spectrophotometer (Halo, DB-20) was used to determine the plasmonic properties of gold nanostars. The absorbance spectrum of the AuNSs was measured in a wavelength range of 400-900 nm. For sample preparation, the pellets of AuNSs were sonicated for 10 minutes in an ultrasonic bath (Huanghua Faithful Instrument Co., Ltd., FSF-010S). The liquid colloidal solution of AuNSs was then transferred to cuvettes and sent to the Environment and Agriculture Lab (SINES) and Commercial Testing, (IESE), SCEE, NUST to obtain absorption spectrum of gold nanostars.

3.5.2 Attenuated Total Reflectance - Fourier-transform Infrared Spectroscopy (ATR-FTIR)

ATR-FTIR spectrometer (Agilent, Cary 630) was used for the identification of the thiol groups on the glass slides. ATR-FTIR spectra was obtained for the glass slides functionalized with MPTMS. The absorption spectra was measured in a range of 400-4000 cm^{-1} wavenumber to determine the presence of certain groups and bonds such as thiol (SH) and Si-OH.

3.5.3 Scanning Electron Microscopy (SEM)

Scanning Electron Microscope (TESCAN, MIRA3) of the Institute of Space and Technology (IST), Islamabad was used to determine the shape, size, and morphology of gold nanostars. For the sample preparation, the colloidal solution of AuNSs was converted to a powdered form. The parameters that were set before analyzing our sample are as follows: 10.00 beam intensity (BI) & 10kV SEM high voltage (HV). The AuNSs were checked on various scales; 500 nm, 200 nm, 1 μm & 2 μm . The sample was seen under different magnifications; 150,000x, 100,000x, 70,000x, 50,000x & 25,000x.

3.5.4 Surfaced Enhanced Raman Spectroscopy (SERS)

SERS spectra of the samples were recorded using a Raman spectrometer (TechnoSpecs Technologies Pvt. Ltd., uRaman-532 TEC-Ci). The wavenumber range (Raman shift) of the Raman spectrometer for our samples ranged from 600 to 1600 cm^{-1} . Moreover, the other

parameters set were 50mW power, 532.4 nm laser wavelength and the acquisition time was varied from 3000-7000 ms to get the best possible results.

4. RESULTS

4.1 SERS Substrate Formation Conformation

4.1.1 UV-Vis Analysis

The UV-Vis absorption spectra graphs for the AuNSs colloidal solution was obtained by UV-VIS spectrophotometer. In order to optimize the shape and plasmonic properties of nanostars, many batches of gold nanostars were prepared and their subsequent absorption spectra were recorded.

Fig. 8 shows the UV-Vis absorption versus wavelength graph of gold nanostars with a broad peak in the range of 600 nm – 700 nm where maximum absorbance was observed at 664 nm wavelength which corresponded with the results mentioned in literature for absorption spectra of gold nanostars (Phiri et al., 2019).

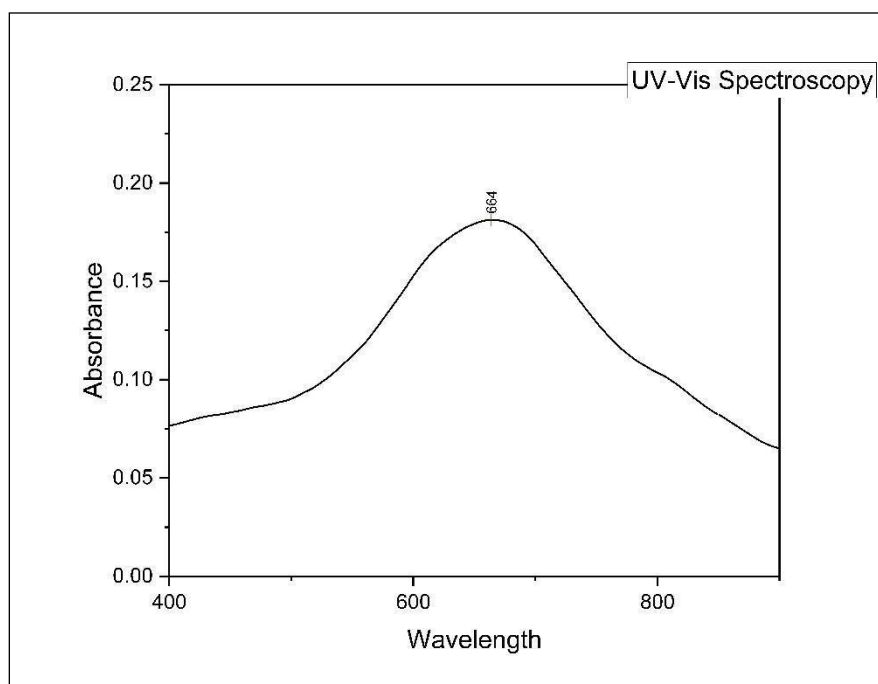


Figure 8 UV-Vis absorption versus wavelength graph of gold nanostars with a broad absorbance peak at 664nm.

4.1.2 Scanning Electron Microscopy (SEM) Analysis

Scanning Electron microscopy was performed to examine the topography and composition of AuNSs. SEM images showed characteristic sharp 3D branches of gold nanostars on different magnifications; 500nm, 200nm, 1 μ m and 2 μ m as shown in Fig. 9 (a) & (b).

The Energy-Dispersive X-ray Spectroscopy (EDS) analysis also confirmed the presence of gold atoms (Au) as shown in Fig. 9 (c). Along with gold, silicon (Si) & oxygen (O) atoms were also present. The existence of silicon was justified as the gold nanostars (powdered form) were placed on the glass slide for the microscopy. Moreover, the glass slide is made of siloxane linkage which validated the presence of oxygen in the sample.

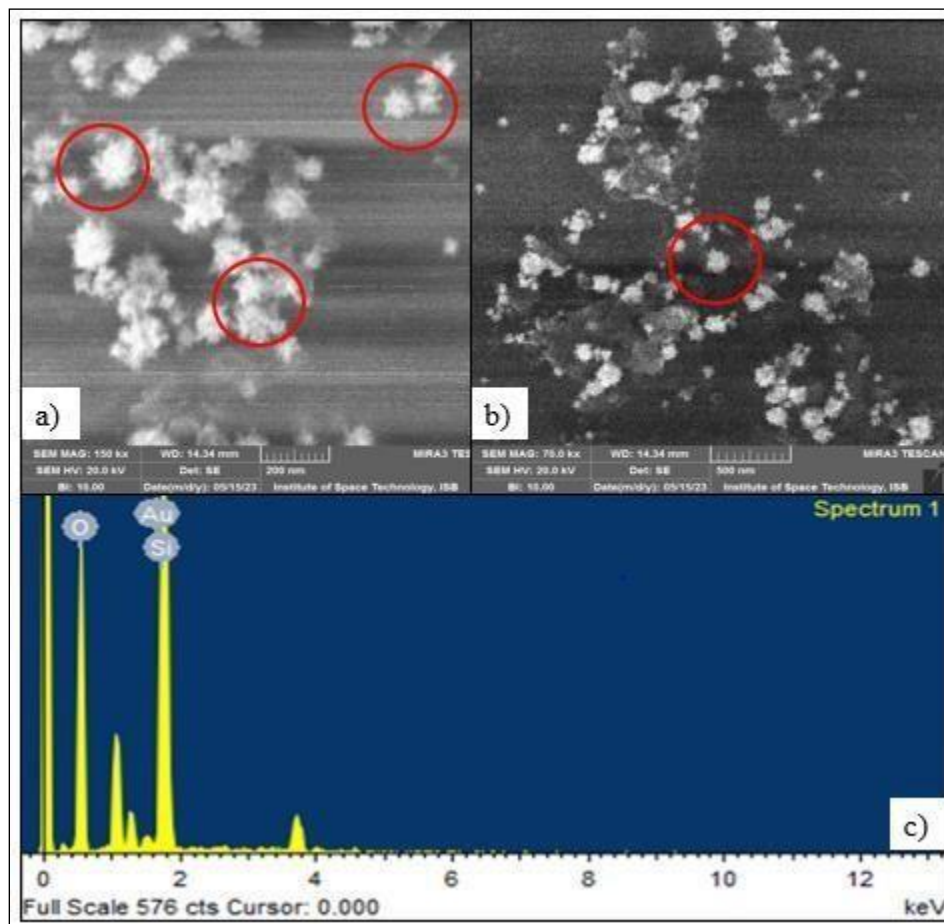


Figure 9 SEM images of gold nanostars where nanostars can be clearly seen in red circles having several branches and tips (a) Magnification 150 kx, scale 200nm. (b) Magnification 70.0 kx, scale 500 nm. (c) EDS analysis of powdered gold nanostars where Au confirms the presence of gold and Si and O correspond to the glass slide.

4.2 Confirmation of Glass Slide Functionalization with Thiol Groups

4.2.1 ATR-FTIR Analysis

ATR-FTIR spectra was obtained for the glass slides functionalized with MPTMS. The FTIR graph for MPTMS functionalized glass slide depicted vibrational peaks in different ranges.

Fig. 10 demonstrates the peaks in the ranges of $700\text{ cm}^{-1} - 800\text{ cm}^{-1}$, $900\text{ cm}^{-1} - 1000\text{ cm}^{-1}$, $1600\text{ cm}^{-1} - 1700\text{ cm}^{-1}$, $2900\text{ cm}^{-1} - 3000\text{ cm}^{-1}$ & $3100\text{ cm}^{-1} - 3500\text{ cm}^{-1}$. A sharp peak split was observed in the range of $900\text{ cm}^{-1} - 1000\text{ cm}^{-1}$ which indicated the presence of siloxane functional group (Si-O-Si) whereas the peak in the $700\text{ cm}^{-1} - 800\text{ cm}^{-1}$ range was relatively less sharp than the aforementioned range. A slight peak noted in the $1600\text{ cm}^{-1} - 1700\text{ cm}^{-1}$ range which exhibited the presence of water. A broad vibrational band was noticed in the $3100\text{ cm}^{-1} - 3500\text{ cm}^{-1}$ range thereby exhibiting silanol functional group (Si-OH). The slight spike observed in the range of $2900\text{ cm}^{-1} - 3000\text{ cm}^{-1}$ displayed C-H stretching of MPTMS.

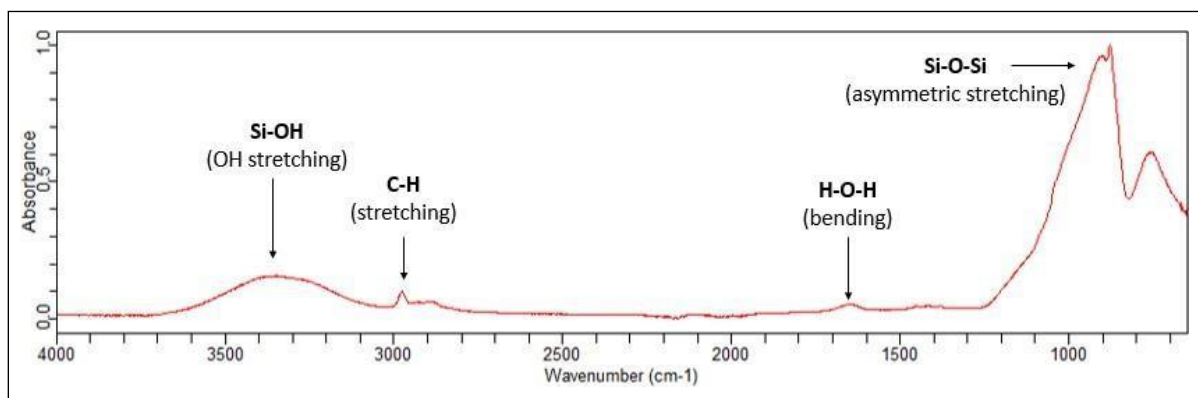


Figure 10 FTIR analysis of MPTMS functionalized SiO₂ glass slides depicting different functional groups and bond stretching.

4.3 Surface Enhanced Raman Spectroscopy (SERS) Analysis

4.3.1 SERS Spectra of Probe Modified Gold Nanostars Adsorbed Slide

To characterize unique Raman spectral features of probe, SERS analysis in a wavelength range of $400\text{ nm} - 1600\text{ nm}$ was carried out using Raman Spectrometer at an excitation wavelength of 532.4 nm to confirm the attachment of probe to gold nanostars. SERS spectra showed a sharp characteristic peak at 1083.89 cm^{-1} as shown in Fig. 11. This peak is attributed to stretching

vibration of C-S bond confirming the attachment of thiolated probe onto the gold nanostars surface through the covalent interaction between Au-S.

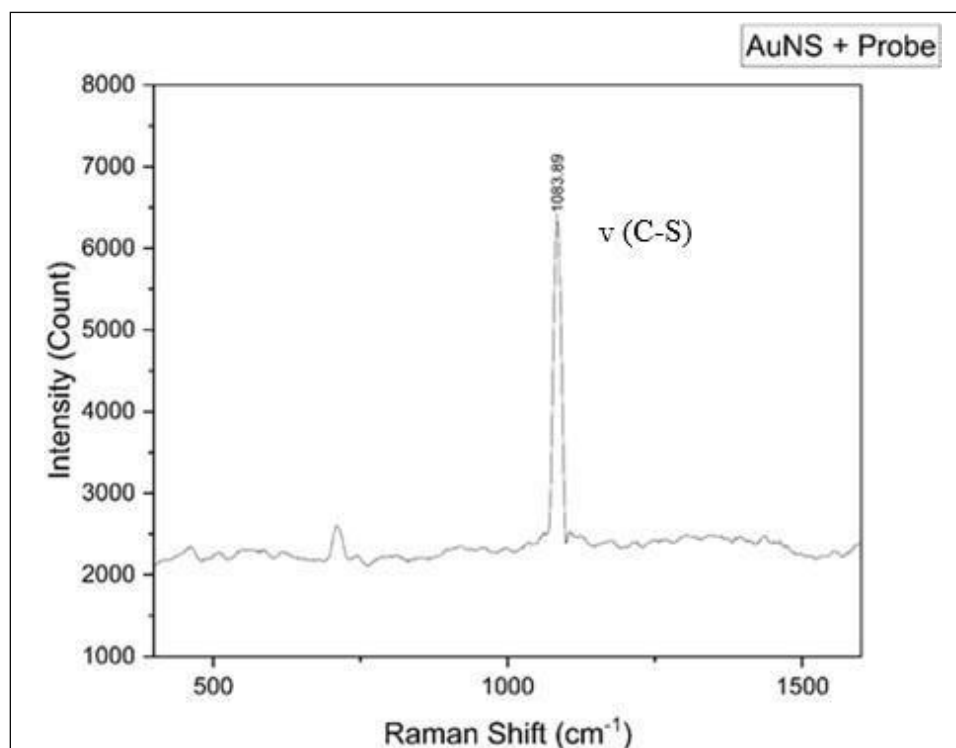


Figure 11 SERS spectra of thiolated ss TB DNA probe modified gold nanostars in a wavelength range of 400-1600 cm^{-1} , indicating a sharp peak at 1083.89 cm^{-1} . The notation ν represents vibration stretching mode of C-S bond.

4.3.2 Comparative SERS Analysis for Analyte Detection

To test the performance of our SERS chip, a comparative analysis for analyte detection was conducted with and without SERS substrate. For this, in addition to measuring SERS signal of analyte attached to thiolated ss probe modified gold nanostars SERS chip, a Raman analysis of analyte attached to probe on a simple glass slide without being aided with gold nanostars was carried out. Both of these measurements were carried out at an excitation wavelength of 532.4 nm in a wavelength range of 600-1600 cm^{-1} .

Fig. 12 (a) shows the graph obtained for SERS analysis where the target analyte is drop casted on the surface of thiolated probe modified gold nanostars whereas Fig. 12 (b) shows the Raman analysis of analyte bonded to probe (i.e., in the absence of gold nanostars). The different peaks in the graphs were attributed to the changes in frequencies of Raman bands resulting from

complimentary DNA binding of analyte and single-stranded probe. However, it is note-worthy that in case of SERS spectra Fig. 12 (a), the Raman intensity for the highest peaks was in a range of 6000-6500 cm^{-1} whereas in Fig. 12 (b) it can be clearly seen that the Raman intensity for the highest peak was in 4000-4500 cm^{-1} range which therefore confirms that Raman signal is enhanced manifold by using unique plasmonic properties of SERS substrates.

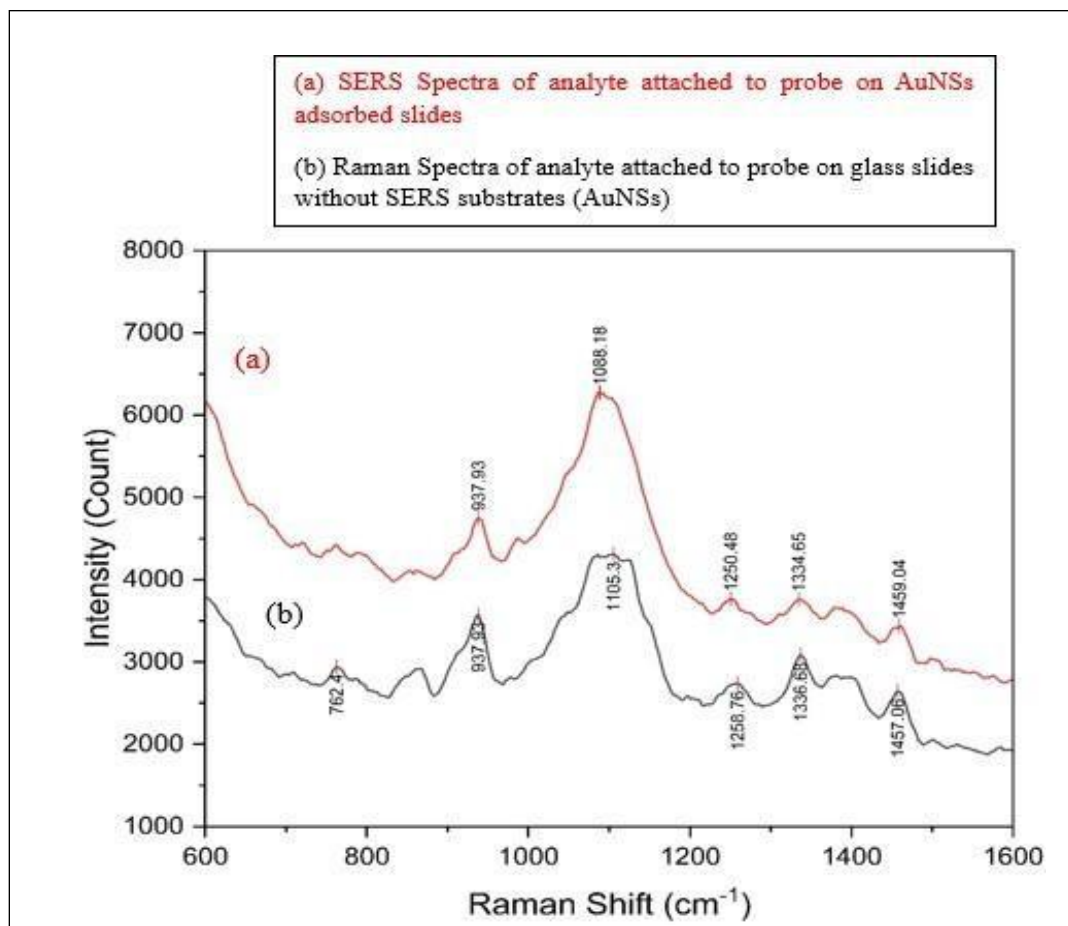


Figure 12 Raman spectra of analyte attached to ss thiolated probe acquired on (a) gold nanostars substrate (SERS Analysis) (b) simple glass slide without SERS substrate (Raman Analysis). The Raman intensity was effectively enhanced by using gold nanostars substrate (6000-6500 cm^{-1}) which results in sensitive detection compared to that obtained without using gold nanostars as substrate (4000-4500 cm^{-1}).

4.3.3 Specificity of SERS DNA Biosensor

In order to evaluate specificity of SERS sensor for TB DNA, an interference experiment was conducted where *E. coli* DNA was used as an analyte for thiolated probe modified gold nanostars SERS chip. SERS analysis was carried out for target analyte (TB DNA) as shown in Fig. 12 (a)

and non-target analyte (*E. coli* DNA) as shown in Fig. 12 (b) individually on the SERS chip and their Raman intensities were independently measured at 1090cm^{-1} and then compared. As shown in Fig. 12 (a) only TB DNA was found to profoundly enhance the Raman intensity whereas *E. coli* DNA showed negligible response. This Fig. 12 graph therefore, clearly depicts that the SERS sensor developed was highly specific and had a great potential for specifically measuring desired analyte (TB DNA) as compared to *E. coli* DNA.

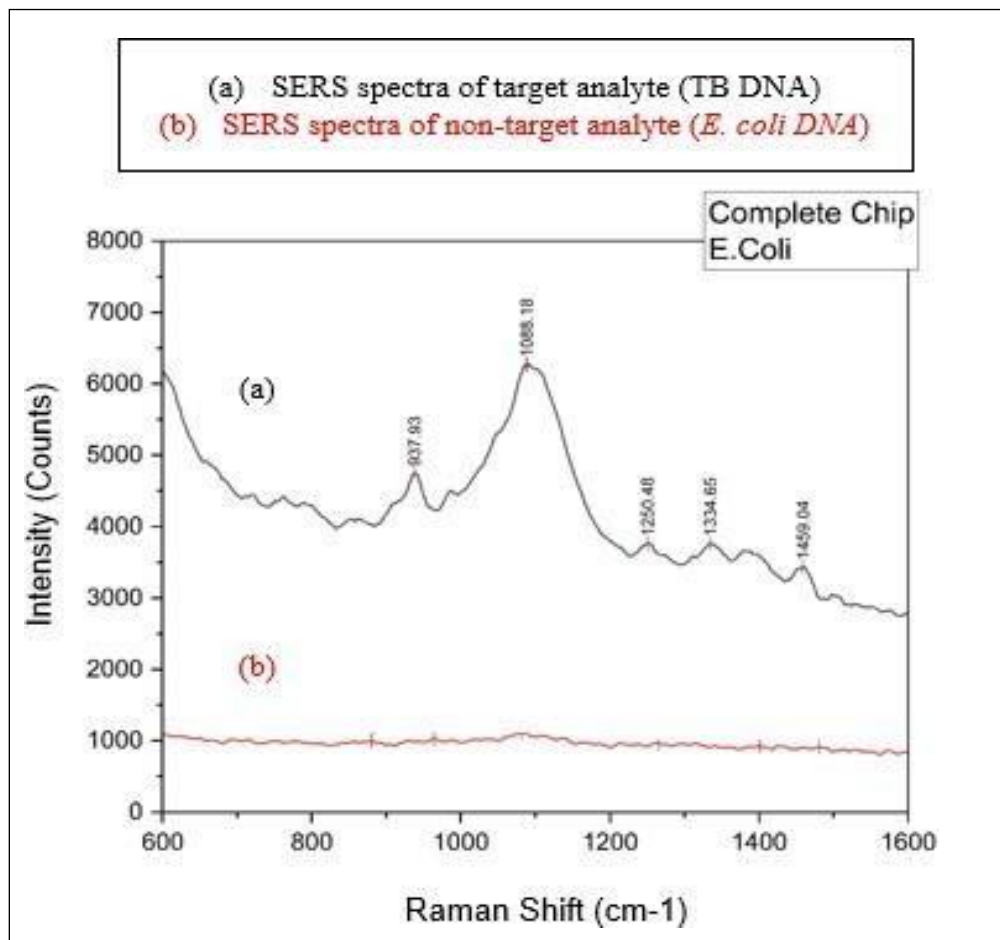


Figure 13 Specificity of thiolated ss DNA probe modified gold nanostars sensor towards TB DNA versus *E. coli* DNA. *E. coli* DNA showed no peaks whereas TB DNA provided enhanced Raman signal as evident by high Raman intensity.

5. DISCUSSION

In this study, gold nanostars were used to develop a simple biosensor for rapid detection of TB DNA by light-driven technology i.e., Surface Enhanced Raman Scattering (SERS). The main goal was to explore the optical properties of gold nanostars to efficiently serve as SERS substrate that could not only result in specific detection of TB but also profoundly enhance the SERS signal.

In this quest, gold nanostars were synthesized following the seed mediated protocol. All the glassware was washed with aqua regia before every batch formation to reduce the maximum level of contamination. Approximately, 20-22 batches of nanostars were made following the protocol cited in methodology in the pursuit to obtain the best possible star conformation. After several tries of optimization, we were able to get the desirable deep blue color of gold nanostar solution and suitable UV results.

The **UV-Vis absorption spectra** result depicted a characteristic broad peak in the range of 600 nm – 700 nm with maximum absorbance at 664 nm wavelength as shown in the Fig. 8. After a thorough literature search and comparing our graph with the available scientific shreds of evidence, it was implied that this peculiar peak at 664 nm in Fig. 8 confirms the presence of moderate-sized seeded AuNSs in the deep blue-colored colloidal solution (Phiri et al., 2019). This peak had a high absorbance of 0.17 AU which means the gold electrons in the conduction band oscillated altogether when the light was bombarded on them. Gold nanostars got excited by the light and showed absorbance at 664 nm following the surface plasmon resonance (SPR) phenomenon.

In order to carry out the conjugation of gold nanostars onto the silica glass slide, MPTMS was used to bind the stars with the slide. As gold cannot bind with the Si-O-Si on glass directly therefore –SH groups of MPTMS were used for linkage purposes. To confirm the functionalization of glass slides, they were subjected to ATR-Fourier Transformed Infrared Spectrometer which analyzed the functional group existence on solid surfaces.

There are two types of graphs that could be obtained after carrying out Fourier Transformed Infrared Spectroscopy; the Transmittance graph and the Absorbance graph. The major difference noticed in both graphs is that the transmittance graph has its peaks facing downward whereas the absorbance graph has its peaks facing upwards. There are several advantages which absorbance graphs of FTIR have over the transmittance graphs. Firstly, understanding the upward-facing

graphs is easier than understanding the graphs facing downward. The second critical reason is that the upward-facing graphs have more tendency to detect low signals when present next to the strong signals which in the case of downward-facing graphs is neglected (Legrand, et al., 2014).

ATR- FTIR graphs as shown in Fig. 10 exhibited absorbance on the y-axis and wavenumber measured in cm^{-1} on the x-axis. The range of the absorbance mentioned was 0.0 – 1.0 whereas the range of the wavenumber stated was $700 \text{ cm}^{-1} - 4000 \text{ cm}^{-1}$. Previous studies demonstrated the presence of a pure mixture of silica-containing siloxane with FTIR peaks at 1057 cm^{-1} & 783 cm^{-1} and Si-O-Si bond peaks at 1033 cm^{-1} (Haider et al., 2022; Nedeljko et al., 2016) The pure thiol group sample shows FTIR peaks at $2500 \text{ cm}^{-1} - 2600 \text{ cm}^{-1}$. But when the FTIR of the sample containing $\text{SiO}_2\text{-SH}$ was done, it highlighted peaks in different ranges of $700 \text{ cm}^{-1} - 800 \text{ cm}^{-1}$, $900 \text{ cm}^{-1} - 1000 \text{ cm}^{-1}$, $1600 \text{ cm}^{-1} - 1700 \text{ cm}^{-1}$, $2900 \text{ cm}^{-1} - 3000 \text{ cm}^{-1}$ & $3100 \text{ cm}^{-1} - 3500 \text{ cm}^{-1}$ as mentioned in the Fig. 10. The peaks generated in the ranges of $700 \text{ cm}^{-1} - 800 \text{ cm}^{-1}$ & $900 \text{ cm}^{-1} - 1000 \text{ cm}^{-1}$ in Fig. 10 confirmed the presence of the *Si-O-Si bond* in the sample. These SiO_2 peaks were very sharp as compared to other peaks presented in the graph. This sharpness indicated how intense the peak was and how much light had been absorbed by the Si-O-Si bonds. Moreover, this peak also depicted the increased asymmetric stretching of the Si-O-Si bonds in the sample which indicated the presence of this bond in greater quantities. The peak generated in the range of $3100 \text{ cm}^{-1} - 3500 \text{ cm}^{-1}$ (alcohol region) in Fig. 10 was a broad vibration peak which indicated the presence of Si-OH bonds. This peak was formed due to the stretching of -OH bonds during the FTIR analysis. The absorbance of this peak was comparatively higher than other peaks except for the SiO_2 peak which was exceptionally high. The peak generated in the range of $1600 \text{ cm}^{-1} - 1700 \text{ cm}^{-1}$ in Fig. 10 showed the presence of H_2O molecules in the sample. The peak's absorbance was < 0.1 confirming the minute levels of water on the glass slide sample. The vibration peak generated in the range of $2900 \text{ cm}^{-1} - 3000 \text{ cm}^{-1}$ in Fig. 10 showed the presence of the C-H bonds. This vibration band proved the presence of MPTMS on the glass slide as C-H bonds are only present in the structure of MPTMS and not in the structure of the glass slide which was silica based.

It is to note that all the demonstrations of the FTIR graph were done after comparing our graph's vibrational bands with the literature (Nedeljko et al., 2016). It is advised that if the FTIR protocol mentioned in this thesis is adapted, one must run the FTIR characterization test a couple of times to achieve the desired results. Changing the protocol also helps in many cases.

Later, SERS analysis was done after attaching probe to gold nanostars adsorbed glass slides. Basically, the attachment of thiolated probe to the gold nano stars occurs through a process called chemisorption, also known as Thiolate-Au bonding. As it has been reported in the literature that metallic nanoparticles, especially gold have strong natural affinity towards thiol group, therefore, thiols chemisorb onto the gold surface forming strong sulfur metallic bond. Therefore, to attach probe (single stranded DNA sequence complimentary to TB) onto the metallic surface, a linkage moiety S-H (mercaptan group) is attached to the probe and then this modified thiolated probe is chemisorbed onto the gold nano stars surface. During this adsorption, electron transfer takes place between the sulfur atom of the thiol group and the gold nano star surface, leading to the formation of negatively charged thiolate species (S^-) and positively charged gold atoms on the surface. This nucleophilic thiolate sulfur atom donates a lone pair of electrons to the gold atoms resulting in the formation of stable C-S covalent bond.

The **SERS graph of complete chip** as shown in the Fig. 11, the peak at 1083 cm^{-1} depicts the stable C-S covalent bond formation between the thiolated probe and the gold nano stars as the literature review confirms the peak range $1000\text{-}1100\text{ cm}^{-1}$ is ideal for C-S bond formation. This covalent C-S bond formed between the thiol group and the gold nano star surface is relatively strong, providing robust attachment of the thiolated molecules to the gold surface. In Fig. 11, the Au-S bonds are indicated by Raman peaks corresponding to the stretching vibrations of C-S bonds. Thus, the peak formation at 1083 cm^{-1} in Fig. 11 provides valuable information about the chemisorption of thiolated probe onto the gold nanostars surface.

For analyte detection purposes, particularly the analysis of Tuberculosis DNA in light of the objective of our research, SERS spectra of TB DNA using gold nanostar as potential SERS substrates was analyzed. When gold nanostars coated glass slides were functionalized with specific DNA probe complimentary to TB DNA sequence, this specific DNA hybridization led to a change in the SERS Spectra that provided sensitive and selective detection. Hybridization of the DNA probe with the targeted DNA caused shifts in the frequencies of Raman Bands corresponding to specific vibrational modes. These shifts were attributed to the chemical interactions between the TB DNA and gold nanostar surface. This binding of TB DNA to the nanostar surface affected the intensity of Raman Spectra. The strong electromagnetic field at the tips of nanostars amplified SERS spectra facilitating detection sensitivity.

The **SERS spectra of TB DNA with SERS substrate** (gold nanostars) is shown in the Fig. 12 (a). The peaks obtained for TB DNA using gold nanostars at 1088.18 cm^{-1} shows enhancement in the intensity of Raman signal as the change in intensity was observed at 6000-6500 counts as shown in Fig. 12 (a). The SERS spectra of TB DNA without SERS substrate (gold nanostars) shows the Raman signaling at an intensity of 4000-4500 counts as depicted by Raman spectra in the Fig. 12 (b). This increase in the intensity of SERS spectra in Fig. 12 (a) justifies the potential capacity of gold nanostars to enhance the SERS detection sensitivity.

Furthermore, SERS signal is highly influenced by the quantity of DNA strands in the sample, the content of four DNA bases and is also affected by the different concentration of bases. Label-free SERS detection involves the hybridization process in which conformational changes in thiol modified DNA probe attached to the metal surface takes place and thereby affecting SERS Spectra. The complimentary DNA probe is a single-stranded DNA base sequence and the SERS spectra of these bases indicate the DNA hybridization process. The SERS Spectra of four DNA bases are due to their distinct vibrational modes associated with molecular structures. SERS spectra of most of the DNA strands is dominated by adenine which exhibits a strong signal at 736 cm^{-1} (Pyrak et al., 2019).

Scientific literature shows that the raman peaks of adenine base that correspond to vibrational modes such as ring breathing, C-N stretching, and ring stretching typically show around $730\text{--}750\text{ cm}^{-1}$, 1240 cm^{-1} , and $1000\text{--}1700\text{ cm}^{-1}$ respectively. The SERS spectrum of thymine often displays Raman peaks around $710\text{--}740\text{ cm}^{-1}$, $1500\text{--}1600\text{ cm}^{-1}$, and 1670 cm^{-1} associated with vibrational modes such as ring breathing, ring stretching, and C=C stretching in the guanine molecule. (Pyrak et al., 2019). Similarly, cytosine shows Raman peaks around $670\text{--}690\text{ cm}^{-1}$, $1510\text{--}1570\text{ cm}^{-1}$, and the C=O stretching mode at around $1,680\text{ cm}^{-1}$ (Pyrak et al., 2019). Guanine is the fourth DNA base and has its own unique Raman peaks in the SERS spectra. Notable peaks for guanine include the ring stretching mode at around $1,500\text{--}1,600\text{ cm}^{-1}$, the C=O stretching mode at around $1,670\text{ cm}^{-1}$, and the ring breathing mode at around $720\text{--}760\text{ cm}^{-1}$ (Pyrak et al., 2019).

SERS graph peaks observed at 762 cm^{-1} in Fig. 12 (b) contributed to the purine rings breathing mode and the peak at 1334 cm^{-1} in Fig. 12 (a) was due to the pyrimidine rings breathing mode. Moreover, the peak at 1250 cm^{-1} in Fig. 12 (a) was attributed to the stretching vibration of the

phosphate groups in the DNA backbone due to the stretching motion of the phosphodiester bonds between adjacent nucleotides.

In a recent study to develop a SERS sensor for detection of melamine in milk, the specificity of sensor was checked by comparing it to other components of milk (Lou et al., 2011). To check the specificity of our SERS biosensor for TB DNA detection, we compared it with another microbial DNA that was used as a control as shown in the Fig. 13. In our research, *E. coli* DNA was labelled as a control group.

A SERS biosensor designed for detecting TB DNA may not necessarily detect *E. Coli* DNA with high specificity due to complimentary probe sequences. This is because the DNA sequences of *Mycobacterium tuberculosis* and *E. coli* bacteria are different since they are two different species of bacteria. Therefore, when our SERS biosensor with adsorbed DNA probe complimentary to the target TB DNA was used to detect SERS spectra of *E. coli* DNA, it resulted in **no SERS spectra** as evident in Fig. 13. To detect *E. coli*, designing specific probes complimentary to *E. coli* DNA is necessary to get highly enhanced SERS response. Therefore, these results show the highly specific nature of SERS Biosensor against the targeted DNA of interest for TB detection.

In the light of our conducted research, it is demonstrated that the highly sensitive SERS signals due to the plasmonic properties of nanostructures can be exploited and used to fabricate specific and sensitive SERS sensors for biosensing and diagnostic purposes. SERS sensors hold tremendous potential for various applications. By carefully designing the sensor, and optimizing numerous factors such as nanostructures shape, size, type, surface properties, attachment to solid surfaces, analyte adsorption, laser power and excitation wavelength of Raman spectrometer, it is possible to achieve high specificity and sensitivity for the detection of target analytes. However, SERS still needs to be explored and continuous developments are required in SERS technology and sensor engineering which will pave way for generating even more potent and versatile SERS sensors in the future.

6. CONCLUSION

Diagnosis is a pre-requisite for the eradication of infectious diseases. Many conventional diagnostic methods in the market fulfill the criteria of efficient diagnosis to some extent with major limitations in sensitivity and specificity; moreover, they are time-consuming. The continuous advancement of research and utilization of contemporary techniques has paved the way for the development of effective biosensors capable of timely diagnosis and treatment of tuberculosis in affected individuals. A wide range of diagnostic tools, both existing and under rapid development, are focused on detecting tuberculosis. The primary emphasis of this research is centered on comprehending cutting-edge biosensor technology in conjunction with nanotechnology to enhance the sensitivity of detection.

Among the light driven technologies, SERS has emerged the most promising techniques to detect trace amounts of biological molecules such as DNA, proteins or even micro RNAs. The unique advantages of SERS, including its high sensitivity, specificity, and label-free detection capabilities, make it an attractive platform for accurate and rapid detection of TB DNA. SERS substrates can efficiently enhance Raman signals manifold creating a powerful biosensor.

The gold nanostars synthesized in our research using seeded protocol were adsorbed on the MPTMS functionalized glass slides and on which TB DNA probes were attached. The SERS spectra obtained from the interaction between the DNA probes and TB DNA provide valuable information for the identification and quantification of TB, contributing to early diagnosis and effective management of the disease. The addition of target and non-target analytes demonstrated the specificity of our SERS sensor for target TB DNA analyte.

Through our conducted series of experiments, we therefore conclude that the morphology and plasmonic properties of gold nanostars enable them to serve as an efficient, highly effective SERS substrate. Thus, gold nanostars based SERS biosensor is a prominent, specific, and sensitive peculiar analytical tool for rapid detection of TB compared to the conventional diagnostic methods available in market.

7. FUTURE PROSPECTS

Future research can aim to further enhance the selectivity and specificity of gold nanostars SERS biosensors for TB DNA detection. Evaluating SERS spectra at different concentrations of TB DNA can help establish the lower limit of detection and determine the linear range of the biosensor.

Future efforts can also be directed towards enhancing the reproducibility of proposed biosensor. This can involve improving the uniformity and consistency of the nanostars' fabrication process, as well as developing standardized protocols for sample preparation and measurement. Furthermore, by minimizing variability in the SERS signals, the biosensor's performance can be enhanced thus making it more reliable and consistent.

Future studies can also focus on understanding the impact of shelf life on the sensitivity of gold nanostars SERS biosensors. Shelf life involves investigating the stability of the nanostars' morphology, surface properties, and signal enhancement capabilities over extended periods and therefore is an important consideration for any biosensor. Ensuring that the biosensor retains its sensitivity throughout its shelf life can provide accurate and consistent results during its intended use.

Moreover, the selection and optimization of Raman reporter molecules play a crucial role in the sensitivity and specificity of SERS biosensors. Future prospects can focus on identifying and designing reporter molecules that exhibit strong Raman scattering signals and high affinity for TB DNA. By fine-tuning the properties of the reporter molecules, such as their Raman-active groups, binding affinity, and stability, the SERS signal can be maximized, leading to improved sensitivity for TB DNA detection.

8. REFERENCES

- Bellah, M. M., Christensen, S. M., & Iqbal, S. M. (2012). Nanostructures for medical diagnostics. In *Journal of Nanomaterials* (Vol. 2012). <https://doi.org/10.1155/2012/486301>
- Betz, J. F., Yu, W. W., Cheng, Y., White, I. M., & Rubloff, G. W. (2014). Simple SERS substrates: Powerful, portable, and full of potential. In *Physical Chemistry Chemical Physics* (Vol. 16, Issue 6). <https://doi.org/10.1039/c3cp53560f>
- Botta, R., Chindaudom, P., Eiamchai, P., Horprathum, M., Limwichean, S., Chananonnawathorn, C., Patthanasettakul, V., Kaewseekhao, B., Faksri, K., & Nuntawong, N. (2018). Tuberculosis determination using SERS and chemometric methods. *Tuberculosis*, 108. <https://doi.org/10.1016/j.tube.2017.12.008>
- Butler, H. J., Ashton, L., Bird, B., Cinque, G., Curtis, K., Dorney, J., Esmonde-White, K., Fullwood, N. J., Gardner, B., Martin-Hirsch, P. L., Walsh, M. J., McAinsh, M. R., Stone, N., & Martin, F. L. (2016). Using Raman spectroscopy to characterize biological materials. *Nature Protocols*, 11(4). <https://doi.org/10.1038/nprot.2016.036>
- Caliendo, A. M., Gilbert, D. N., Ginocchio, C. C., Hanson, K. E., May, L., Quinn, T. C., Tenover, F. C., Alland, D., Blaschke, A. J., Bonomo, R. A., Carroll, K. C., Ferraro, M. J., Hirschhorn, L. R., Joseph, W. P., Karchmer, T., MacIntyre, A. T., Reller, L. B., Jackson, A. F., & Infectious Diseases Society of America (IDSA). (2013). Better tests, better care: improved diagnostics for infectious diseases. In *Clinical infectious diseases: an official publication of the Infectious Diseases Society of America: Vol. 57 Suppl 3*. <https://doi.org/10.1093/cid/cit578>
- Chakaya, J., Khan, M., Ntoumi, F., Aklillu, E., Fatima, R., Mwaba, P., Kapata, N., Mfinanga, S., Hasnain, S. E., Katoto, P. D. M. C., Bulabula, A. N. H., Sam-Agudu, N. A., Nachega, J. B., Tiberi, S., McHugh, T. D., Abubakar, I., & Zumla, A. (2021). Global Tuberculosis Report 2020 – Reflections on the Global TB burden, treatment and prevention efforts. *International Journal of Infectious Diseases*, 113. <https://doi.org/10.1016/j.ijid.2021.02.107>
- Cong, S., Liu, X., Jiang, Y., Zhang, W., & Zhao, Z. (2020). Surface Enhanced Raman Scattering Revealed by Interfacial Charge-Transfer Transitions. In *Innovation* (Vol. 1, Issue 3). <https://doi.org/10.1016/j.xinn.2020.100051>

- Deng, J., Dong, J., & Cohen, P. (2018). *Rapid Fabrication and Characterization of SERS Substrates*. 26. <https://doi.org/10.1016/j.promfg.2018.07.068>
- De Silva Indrasekara, A. S., Johnson, S. F., Odion, R. A., & Vo-Dinh, T. (2018). Manipulation of the Geometry and Modulation of the Optical Response of Surfactant-Free Gold Nanostars: A Systematic Bottom-Up Synthesis. *ACS Omega*, 3(2). <https://doi.org/10.1021/acsomega.7b01700>
- Edinburgh Instruments Ltd. (2023). Surfaced Enhanced Raman Scattering (SERS) | Edinburgh Instruments. <https://www.edinst.com/us/blog/surfaced-enhanced-raman-scattering-sers/>
- Feynman, R. P. (1992). There's plenty of room at the bottom. *Journal of Microelectromechanical Systems*, 1(1). <https://doi.org/10.1109/84.128057>
- Filip, J., & Tkac, J. (2018). Enzymatic electrodes: Characteristics, fabrication methods, and applications. In *Encyclopedia of Interfacial Chemistry: Surface Science and Electrochemistry*. <https://doi.org/10.1016/B978-0-12-409547-2.13471-7>
- Gothe, P. K., Gaur, D., & Achanta, V. G. (2018). Mptms self-assembled monolayer deposition for ultra-thin gold films for plasmonics. *Journal of Physics Communications*, 2(3). <https://doi.org/10.1088/2399-6528/aaaedd>
- Haider, J. B., Haque, M. I., Hoque, M., Hossen, M., Mottakin, M., Khaleque, A., Johir, M., Zhou, J. L., Jeon, S., & Zargar, M. (2022). Efficient extraction of silica from openly burned rice husk ash as adsorbent for dye removal. *Journal of Cleaner Production*, 380, 135121. <https://doi.org/10.1016/j.jclepro.2022.135121>
- Hamm, L., Gee, A., & Indrasekara, A. S. D. S. (2019). Recent advancement in the surface-enhanced raman spectroscopy-based biosensors for infectious disease diagnosis. In *Applied Sciences (Switzerland)* (Vol. 9, Issue 7). <https://doi.org/10.3390/app9071448>
- Huang, C., Bonroy, K., Reekman, G., Verstreken, K., Lagae, L., & Borghs, G. (2009). An on-chip localized surface plasmon resonance-based biosensor for label-free monitoring of antigen-antibody reaction. *Microelectronic Engineering*, 86(12). <https://doi.org/10.1016/j.mee.2009.05.009>

- Indrasekara, A. S. D. S., Meyers, S., Shubeita, S., Feldman, L. C., Gustafsson, T., & Fabris, L. (2014). Gold nanostar substrates for SERS-based chemical sensing in the femtomolar regime. *Nanoscale*, 6(15). <https://doi.org/10.1039/c4nr02513j>
- Jianrong, C., Yuqing, M., Nongyue, H., Xiaohua, W., & Sijiao, L. (2004). Nanotechnology and biosensors. *Biotechnology Advances*, 22(7). <https://doi.org/10.1016/j.biotechadv.2004.03.004>
- Kumar, S., Kumar, P., Das, A., & Shakher Pathak, C. (2020). Surface-Enhanced Raman Scattering: Introduction and Applications. In *Recent Advances in Nanophotonics - Fundamentals and Applications*. <https://doi.org/10.5772/intechopen.92614>
- Liang, X., Li, N., Zhang, R., Yin, P., Zhang, C., Yang, N., Liang, K., & Kong, B. (2021). Carbon-based SERS biosensor: from substrate design to sensing and bioapplication. In *NPG Asia Materials* (Vol. 13, Issue 1). <https://doi.org/10.1038/s41427-020-00278-5>
- Liu, X., Guo, J., Li, Y., Wang, B., Yang, S., Chen, W., Wu, X., Guo, J., & Ma, X. (2021). SERS substrate fabrication for biochemical sensing: Towards point-of-care diagnostics. In *Journal of Materials Chemistry B* (Vol. 9, Issue 40). <https://doi.org/10.1039/d1tb01299a>
- Lou, T., Wang, Y., Li, J., Peng, H., Xiong, H., & Chen, L. X. (2011). Rapid detection of melamine with 4-mercaptopyridine-modified gold nanoparticles by surface-enhanced Raman scattering. *Analytical and Bioanalytical Chemistry*, 401(1), 333–338. <https://doi.org/10.1007/s00216-011-5067-3>
- Mosier-Boss P. A. (2017). Review of SERS Substrates for Chemical Sensing. *Nanomaterials* (Basel, Switzerland), 7(6), 142. <https://doi.org/10.3390/nano7060142>
- Nedeljko, P., Turel, M., Ban, I., & Lobnik, A. (2016). Synthesis of hybrid thiol-functionalized SiO₂ particles used for agmatine determination. *Journal of Sol-Gel Science and Technology*, 79(3), 487–496. <https://doi.org/10.1007/s10971-016-4030-3>
- Parmigiani, M., Albin, B., Pellegrini, G., Genovesi, M., De Vita, L., Pallavicini, P., Dacarro, G., Galinetto, P., & Taglietti, A. (2022). Surface-Enhanced Raman Spectroscopy Chips Based on Silver Coated Gold Nanostars. *Nanomaterials*, 12(20). <https://doi.org/10.3390/nano12203609>

- Pérez-Jiménez, A. I., Lyu, D., Lu, Z., Liu, G., & Ren, B. (2020). Surface-enhanced Raman spectroscopy: Benefits, trade-offs and future developments. In *Chemical Science* (Vol. 11, Issue 18). <https://doi.org/10.1039/d0sc00809e>
- Petersen, M., Yu, Z., & Lu, X. (2021). Application of Raman spectroscopic methods in food safety: A review. In *Biosensors* (Vol. 11, Issue 6). <https://doi.org/10.3390/bios11060187>
- Phiri, M. M., Mulder, D. W., & Vorster, B. C. (2019). Seedless gold nanostars with seed-like advantages for biosensing applications. *Royal Society Open Science*, 6(2). <https://doi.org/10.1098/rsos.181971>
- Premasiri, W. R., Moir, D. T., Klempner, M. S., Krieger, N., Jones, G., & Ziegler, L. D. (2005). Characterization of the Surface Enhanced Raman Scattering (SERS) of bacteria. *Journal of Physical Chemistry B*, 109(1). <https://doi.org/10.1021/jp040442n>
- Pyrak, E., Krajczewski, J., Kowalik, A., Kudelski, A., & Jaworska, A. (2019). Surface enhanced raman spectroscopy for DNA biosensors - How far are we? In *Molecules* (Vol. 24, Issue 24). <https://doi.org/10.3390/molecules24244423>
- Rao, X., Tatouljian, M., Guyon, C., Ognier, S., Chu, C., & Hassan, A. A. (2019). A comparison study of functional groups (amine vs. thiol) for immobilizing AuNPs on zeolite surface. *Nanomaterials*, 9(7). <https://doi.org/10.3390/nano9071034>
- Saviñon-Flores, F., Méndez, E., López-Castaños, M., Carabarin-Lima, A., López-Castaños, K. A., González-Fuentes, M. A., & Méndez-Albores, A. (2021). A review on sers-based detection of human virus infections: Influenza and coronavirus. In *Biosensors* (Vol. 11, Issue 3). <https://doi.org/10.3390/bios11030066>
- Srivastava, S. K., Van Rijn, C. J. M., & Jongsma, M. A. (2016). Biosensor-based detection of tuberculosis. In *RSC Advances* (Vol. 6, Issue 22). <https://doi.org/10.1039/c5ra15269k>
- Weinrib, H., Meiri, A., Duadi, H., & Fixler, D. (2012). Uniformly Immobilizing Gold Nanorods on a Glass Substrate. *Journal of Atomic, Molecular, and Optical Physics*, 2012, 1–6. <https://doi.org/10.1155/2012/683830>
- Wolinsky, E. (1994). Conventional diagnostic methods for tuberculosis. *Clinical Infectious Diseases*, 19(3). <https://doi.org/10.1093/clinids/19.3.396>

Pleg Check

ORIGINALITY REPORT

10%

SIMILARITY INDEX

8%

INTERNET SOURCES

6%

PUBLICATIONS

1%

STUDENT PAPERS

PRIMARY SOURCES

1	pdf-s3.xuebalib.com:1262 Internet Source	1%
2	www.science.gov Internet Source	1%
3	www.mdpi.com Internet Source	1%
4	Agnieszka A. Zuber, Elizaveta Klantsataya, Akash Bachhuka. "Biosensing ☆", Elsevier BV, 2018 Publication	1%
5	www.freepatentsonline.com Internet Source	1%
6	www.qdecor.ro Internet Source	<1%
7	Dorleta Jimenez de Aberasturi, Ana Belén Serrano-Montes, Luis M. Liz-Marzán. "Modern Applications of Plasmonic Nanoparticles: From Energy to Health", Advanced Optical Materials, 2015 Publication	<1%

8	www.esanpedia.oar.ubu.ac.th Internet Source	<1 %
9	hdl.handle.net Internet Source	<1 %
10	link.springer.com Internet Source	<1 %
11	Logan Hamm, Amira Gee, A. Swarnapali De Silva Indrasekara. "Recent Advancement in the Surface-Enhanced Raman Spectroscopy-Based Biosensors for Infectious Disease Diagnosis", Applied Sciences, 2019 Publication	<1 %
12	Wijamunidurage R. Premasiri, Ying Chen, Jennifer Fore, Amy Brodeur, Lawrence D. Ziegler. "SERS Biomedical Applications: Diagnostics, Forensics, and Metabolomics", Elsevier BV, 2018 Publication	<1 %
13	scholarworks.umass.edu Internet Source	<1 %
14	etd.uwc.ac.za Internet Source	<1 %
15	kclpure.kcl.ac.uk Internet Source	<1 %
16	digitalcommons.pace.edu Internet Source	<1 %

40

17	Pietro Strobbia, Tyjair Sadler, Ren A. Odion, Tuan Vo-Dinh. "SERS in Plain Sight: A Polarization Modulation Method for Signal Extraction", Analytical Chemistry, 2019 Publication	<1 %
18	Principles of Bacterial Detection Biosensors Recognition Receptors and Microsystems, 2008. Publication	<1 %
19	ulspace.ul.ac.za Internet Source	<1 %
20	www.lib.kobe-u.ac.jp Internet Source	<1 %
21	Submitted to North West University Student Paper	<1 %
22	Submitted to University of Southampton Student Paper	<1 %
23	Submitted to Taylor's Education Group Student Paper	<1 %
24	pubmed.ncbi.nlm.nih.gov Internet Source	<1 %
25	studentsrepo.um.edu.my Internet Source	<1 %
26	www.mobt3ath.com Internet Source	<1 %

27	Submitted to Manchester Metropolitan University	<1 %
Student Paper		
28	dokumen.pub	<1 %
Internet Source		
29	Bridget M. Crawford, Pietro Strobbia, Hsin-Neng Wang, Rodolfo Zentella et al. "Plasmonic Nanoprobes for in Vivo Multimodal Sensing and Bioimaging of MicroRNA within Plants", ACS Applied Materials & Interfaces, 2019	<1 %
Publication		
30	Chenlu Xie, Yu Wang, Wei Wang, Dan Yu. "Flexible, conductive and multifunctional cotton fabric with surface wrinkled MXene/CNTs microstructure for electromagnetic interference shielding", Colloids and Surfaces A: Physicochemical and Engineering Aspects, 2022	<1 %
Publication		
31	Premasiri, W. Ranjith, Yoseph Gebregziabher, and Lawrence D. Ziegler. "On the Difference Between Surface-Enhanced Raman Scattering (SERS) Spectra of Cell Growth Media and Whole Bacterial Cells", Applied Spectroscopy, 2011.	<1 %
Publication		
32	acadpubl.eu	
Internet Source		

		<1 %
33	eprints.utm.my Internet Source	<1 %
34	ijpsr.com Internet Source	<1 %
35	vdoc.pub Internet Source	<1 %
36	www.prf.upol.cz Internet Source	<1 %
37	zero.sci-hub.se Internet Source	<1 %
38	Shinki, Subhendu Sarkar. "Is 3D surface structuring always a prerequisite for effective SERS?", Surfaces and Interfaces, 2022 Publication	<1 %
39	Tong-Seung Tseng, Winslow R. Briggs. " The Mutation Impairs Dephosphorylation of Phot2, Resulting in Enhanced Blue Light Responses ", The Plant Cell, 2010 Publication	<1 %
40	curve.carleton.ca Internet Source	<1 %
41	pubs.rsc.org Internet Source	<1 %

42	royalsocietypublishing.org Internet Source	<1 %
43	spiral.imperial.ac.uk Internet Source	<1 %
44	www.pcouncil.org Internet Source	<1 %
45	W. H. Baur. "Silicon-oxygen bond lengths, bridging angles Si-O-Si and synthetic low tridymite", Acta Crystallographica Section B Structural Crystallography and Crystal Chemistry, 1977 Publication	<1 %
46	Audrey Sassolas, Béatrice D. Leca-Bouvier, Loïc J. Blum. "DNA Biosensors and Microarrays", Chemical Reviews, 2007 Publication	<1 %
47	Barbara Tymczyna - Borowicz, Jakub Nowak, Maciej Jarzębski, Andrzej Kuczumow. "Elemental and chemical compounds study of enamel and dentine of porcine primary molar teeth", X-Ray Spectrometry, 2019 Publication	<1 %

Exclude quotes Off

Exclude matches Off

Exclude bibliography On